

**METHYLTRANSFERASES AS AGENTS
OF CHEMICAL DIVERSITY**

**METHYLTRANSFERASES AS AGENTS OF CHEMICAL
DIVERSITY IN NATURAL PRODUCTS**

By

BIJAN ZAKERI, H.B.Sc.

A Thesis

Submitted to the School of Graduate Studies

in Partial Fulfilment of the Requirements

for the Degree

Master of Science

McMaster University

© Copyright by Bijan Zakeri, July 2008

Descriptive Note

MASTER OF SCIENCE (2008)

McMaster University

(Chemical Biology)

TITLE: Methyltransferases as Agents of Chemical Diversity in Natural
 Products

AUTHOR: Bijan Zakeri, H.B.Sc. (McMaster University)

SUPERVISOR: Professor Gerard D. Wright

NUMBER OF PAGES: ix, 78

Abstract

The extensive use of antibiotics in the clinic, veterinary medicine, and agricultures has imposed an immense selective pressure for the emergence of antibiotic resistant bacteria. In order to maintain the upper hand against pathogenic bacteria, we must constantly seek new antimicrobials. Most antibiotics used in the clinic were discovered as natural products or are derivatives thereof. Therefore, we must seek means of increasing the chemical diversity of natural products in our quest for new antibiotics. Herein, we investigate methyltransferases as agents to increase chemical diversity. More specificity, we have performed biochemical studies on a tetracycline and a glycopeptide methyltransferase.

In our studies of the putative tetracycline N-methyltransferase OxyT, we determined the conditions required to overexpress the protein in an *E. coli* host. Subsequently, using purified protein we examined substrate specificity using commercially available compounds. However, we were unable to detect methylation of the compounds tested and therefore we made an effort to secure a biologically relevant substrate by insertionally inactivating the *oxyT* gene in *S. rimosus* but were unsuccessful.

In our studies of the glycopeptide N-methyltransferase MtfA, we examined the biochemical activity of this enzyme on the glycopeptide desulfo-A47934. We purified desulfo-A47934 as a fermentation product of *S. toyocaensis* Δ *staL* and determined an extinction co-efficient of $4200 \text{ Lmol}^{-1}\text{cm}^{-1}$. Furthermore, based on a crystal structure of MtfA we biochemically characterized the enzyme and its four mutants Y32F, E144A,

H228A, and R230A to study residues involved in substrate binding and catalysis. We demonstrated that these mutations did not alter quaternary protein structure but did lead to a significant decrease in enzyme activity as compared to the wild-type enzyme.

Acknowledgements

To my supervisor Dr. Gerry Wright, thank you for your support and guidance. You pushed me to always improve and to be a better scientist. Most importantly I would like to thank you for teaching me the scientific method and demonstrating the dedication and sacrifices that are required for becoming a great scientist. I would like to thank my committee members Dr. Fred Capretta and Dr. Justin Nodwell for their insight and helpful advice that always helped me to view my project from a different angle. I would also like to thank Dr. Mirek Cygler, Dr. Allan Matte, and Dr. Rong Shi (National Research Council of Canada) for a successful collaboration.

I would like to dedicate this work to my family and in particular to my mother who was always there to support me in my troubles and there to share in my joys.

Table of Contents

Descriptive Note	ii
Abstract	iii
Acknowledgements	v
Table of Contents	vi
List of Tables and Figures	viii
<u>CHAPTER 1: Introduction</u>	1
1. Introduction	2
1.1. Natural Products	2
1.2. Actinomycetes	3
1.3. Secondary Metabolites	5
1.4. Project Objectives	8
1.5. Methyltransferases	9
Reference List	14
<u>CHAPTER 2: Investigation of A Tetracycline Methyltransferase</u>	16
2.1. Introduction	17
2.2. Materials and Methods	21
2.2.1. Cloning of the <i>oxyT</i> gene	21
2.2.2. Expression and Purification of OxyT	23
2.2.3. OxyT Activity Assays	24
2.2.4. Analytical Gel Filtration of OxyT	25
2.3. Results and Discussion	26
2.4. Conclusions	33
Reference List	35
<u>CHAPTER 3: Investigation of a Glycopeptide Methyltransferase</u>	37
3.1. Introduction	38
3.2. Materials and Methods	41
3.2.1. Amplification and Cloning of <i>mtfA</i> Mutants	41
3.2.2. Purification of MtfA and Its Mutants	42
3.2.3. Purification of desulfo-A47934	43
3.2.4. Determination of Extinction Co-efficient	45
3.2.5. Enzyme Activity Assays	46
3.2.6. Circular Dichroism Analysis of MtfA Wild-Type and Mutants	46
3.2.7. Analytical Gel Filtration of MtfA Wild-Type and Mutants	47
3.3. Results and Discussion	49

3.4. Conclusions	63
Reference List	65
<u>CHAPTER 4: Summary</u>	66
4.1. Summary	67
Appendix	69
Materials and Methods	69
Disruption of the <i>oxyT</i> gene in <i>S. rimosus</i>	69
Electroporation of <i>S. rimosus</i>	71
Results	73
Reference List	78

List of Tables and Figures

CHAPTER 1: Introduction

Table

Table 1.1. Approximate number of antibiotics produced by microbes	3
--	---

Figures

Figure 1.1. Actinomyces colony architecture	4
Figure 1.2. Examples of secondary metabolites produced by actinomycetes	7
Figure 1.3. A typical methyltransferase reaction mechanism	11
Figure 1.4. The core fold of SAM-dependent methyltransferases	12

CHAPTER 2: Investigation of A Tetracycline Methyltransferase

Figures

Figure 2.1. The dimethylation reaction catalyzed by OxyT	20
Figure 2.2. Tetracycline binding to the 30S ribosomal subunit	20
Figure 2.3. Compounds used to test OxyT activity	27
Figure 2.4. OxyT enzymatic assays	29
Figure 2.5. OxyT enzymatic assays analyzed by LC/MS	31
Figure 2.6. Gel filtration analysis of OxyT	32
Figure 2.7. Chemical structures of 4-amino-anhydrotetracycline and chelocardin	34

CHAPTER 3: Investigation of a Glycopeptide Methyltransferase

Tables

Table 3.1. PCR primer details for site-directed mutagenesis on pET28a- <i>mtfA</i>	42
Table 3.2. A summary of the protein standards used to calibrate the Superdex 200 HR 10/30 gel filtration column	48
Table 3.3. Catalytic activity of MtfA wild-type, Y32F, E144A, H228A, and R230A	58
Table 3.4. Calculation of protein molecular weights using a Superdex 200 HR 10/30 gel filtration column	62

Figures	
Figure 3.1. The structures of A47934 and desulfo-A47934	40
Figure 3.2. The methylation reaction catalyzed by MtfA	40
Figure 3.3. Purification of crude desulfo-A47934 by RP-HPLC	50
Figure 3.4. Absorption spectrum of desulfo-A47934	51
Figure 3.5. SAM and desulfo-A47934 bound to the substrate binding site of MtfA	53
Figure 3.6. Wild-type MtfA methylation of desulfo-A47934	54
Figure 3.7. Standard curve of desulfo-A47934 on RP-HPLC measured at 280 nm	55
Figure 3.8. RP-HPLC analysis of desulfo-A47934 methylation by MtfA wild-type and mutants	57
Figure 3.9. Circular dichroism spectrums of MtfA wild-type, Y32F, E144A, H228A, and R230A	60
Figure 3.10. A standard curve of Superdex 200 HR 10/30 gel filtration column	61

Appendix

Figure A.1. Plasmid map of pSTEA	73
Figure A.2. LC/MS analysis of putative <i>oxyT</i> -null <i>S. rimosus</i> mutants	76
Figure A.3. PCR screening of putative <i>oxyT</i> -null <i>S. rimosus</i> mutants	77

CHAPTER 1: INTRODUCTION

This chapter contains published material from the following article:

Zakeri, B., and Wright, G. D. (2008). Chemical biology of tetracycline antibiotics. *Biochem. Cell Biol.*, 86, 124-136.

Methyltransferases as Agents of Chemical Diversity in Natural Products

1. Introduction

1.1. Natural Products

“NATURE! We are surrounded and embraced by her: powerless to separate ourselves from her, and powerless to penetrate beyond her”, as interpreted by T. H. Huxley from aphorisms by Goethe (Huxley, 1869). Nature imposes many challenges to life. Living organisms are constantly in competition with other organisms both great and small. We must constantly compete for life’s necessities, while also dealing with many environmental stresses including those of the biological, physical, and chemical in origin. In light of all of these complex interactions, we carve out niches for ourselves in which we can live in relative harmony. Thus, as humans we have adapted to live with all these challenges and in particular with the microbial life that surrounds us. Yet, not all of our interactions are beneficial or harmless and we have to constantly fend off threats to our well being. In particular, pathogenic bacteria pose one of the greatest threats to our health and can cause disease from isolated cases to pandemics. Through innovative and pioneering scientific work in the past century, we have managed to combat many bacterial infections through the use of antibiotics and vaccines. However, in order to compete with evolution and the power of natural selection, we must constantly seek new antibiotics and complimentary strategies to battle with the pathogenic bacteria that do us harm.

Although our environment exposes us to many bacterial threats, it also provides us with the means to fight back. Microbes have evolved to produce small molecule secondary metabolites that can kill or otherwise arrest the growth of other microbes. These natural products provide us with a vast chemical repertoire that we can exploit for human medicine. As reported by Janos Berdy in 2005, microbes provide us with a tremendous amount of antibiotics that dominate human therapy, of which the majority are derived from the actinomycetes (Table 1.1) (Berdy, 2005).

Table 1.1. Approximate number of antibiotics produced by microbes, which can be practically used in human medicine, veterinary medicine, and agriculture (Berdy, 2005).

Microbial Source	Number of Antibiotics Produced	Practically Used Antibiotics (in Human Therapy)
Actinomycetes	8700	100-120 (70-75)
Other Bacteria	2900	10-12 (8-10)
Fungi	4900	30-35 (13-15)
Total	16500	140-160 (100)

1.2. Actinomycetes

Actinomyces are soil-dwelling filamentous Gram-positive bacteria. These bacteria possess a very complex life-cycle in which filamentous colony growth, sporulation, and secondary metabolite synthesis are intricately regulated. Actinomycetes are indeed a unique group of bacteria and due to their filamentous appearance they phenotypically resemble fungi more so than bacteria. In fact, the term “actinomyces” means “ray

fungus” and was first used by the German botanist Carl Otto Harz in a description of a microorganism that caused disease in cattle (*Actinomyces bovis*) (Hopwood, 2007). The filamentous colony growths of actinomycetes are intricately controlled by a cascade of genes that determine the temporal aspect of colony growth. First, substrate mycelia penetrate into the solid nutrient source and utilize readily available soluble nutrients (Fig. 1.1). Once nutrients become limiting, aerial mycelium begins to grow out the solid medium obtaining nutrients by partially cannibalizing on the substrate mycelium (Chater, 2006; Chater, 1993). Aerial mycelium growth then leads to sporulation. It is during this latter stage of the colony life-cycle that secondary metabolite synthesis begins, where it is believed that antibiotic production will aid aerial mycelium growth and sporulation by protecting the colony from being attacked by competing microorganisms (Chater, 2006).

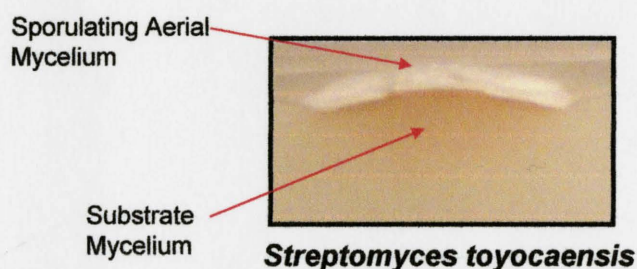


Figure 1.1. Actinomyces colony architecture. Initially colonies are established by primary mycelium growth. Once nutrients become limiting, aerial mycelium formation, sporulation, and secondary metabolite production commences. Shown is a cross-section of *Streptomyces toyocaensis* grown on Bennet agar at 30°C for 3 days.

In accordance with their complex life-cycle and an ability to often produce an array of secondary metabolites, it is not a surprise that actinomycetes possess relatively large genomes as compared to other bacteria. In 2002, the genome of the model actinomycete *Streptomyces coelicolor* A3(2) was sequenced, revealing a single linear genome of ~8.7 Mb with an origin of replication situated in the centre of the chromosome (Bentley et al., 2002). Interestingly, the genome sequence also revealed over 20 gene clusters that could potentially encode for secondary metabolite biosynthesis (Bentley et al., 2002). This array of metabolic programs for natural products has been the hallmark of other sequenced actinomycete genomes including *Saccharopolyspora erythraea* and *Streptomyces griseus* (Oliynyk et al., 2007; Ohnishi et al., 2008). Thus, each actinomycete can potentially offer us several chemical scaffolds that we can exploit for medicinal purposes and we have simply scratched the surface of the potential of these bacteria.

1.3. Secondary Metabolites

Actinomycete biology is an intriguing topic and one that is poorly understood relative to other bacteria. However, over the past several decades we have taken great strides towards better understanding secondary metabolite biosynthesis by actinomycetes. Certain secondary metabolites are produced by single mega-enzyme complexes that function in a ‘conveyor belt’ fashion such as type I polyketide synthases (PKS) and nonribosomal peptide synthetases (NRPS); while others are produced by type II PKSs that function as separate and distinct enzymatic subunits (Zakeri and Wright, 2008; Lai et

al., 2006). These elaborate enzymatic pathways are able to fashion small molecules with varying degrees of complexity based on chemical scaffolds that often possess several chiral centres. The biosynthetic pathways utilize simple building blocks that are readily available in cells such as malonyl-CoA, carbohydrates, and amino acids. These are subsequently assembled into a wide variety of diverse and unrelated structures. Figure 1.2 provides a few examples of natural products to illustrate the chemical complexity of some of these molecules. These chemical scaffolds are often out the reach of medicinal chemists to produce synthetically in useful quantities, which significantly inhibits our ability to increase chemical diversity.

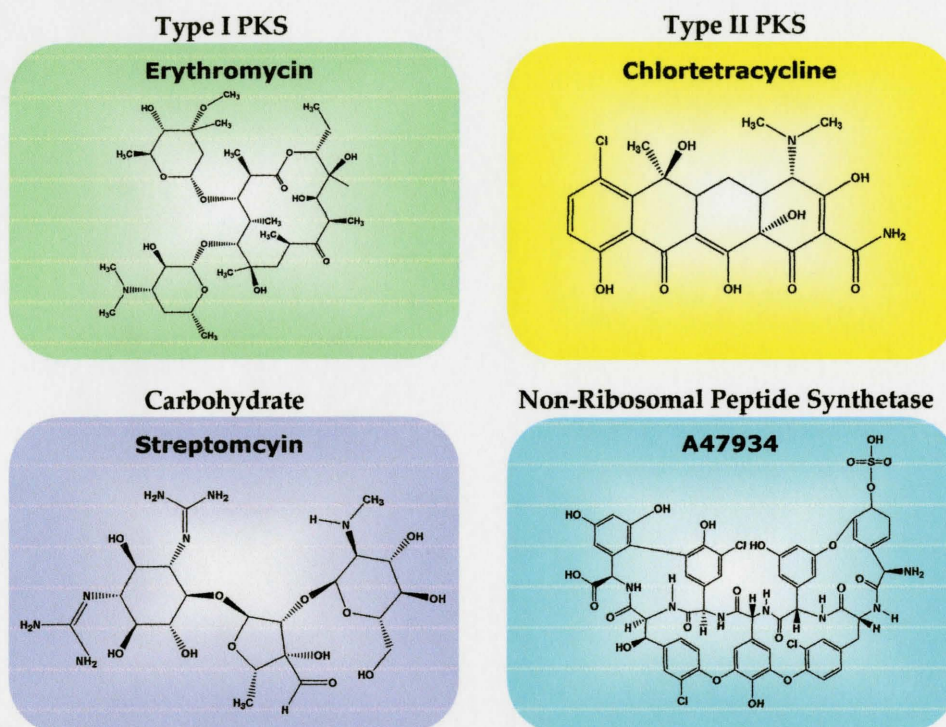


Figure 1.2. Examples of secondary metabolites produced by actinomycetes and the machinery used to produce them. Each of these compounds possesses a complex chemical structure with several chiral centres. This makes their chemical synthesis very challenging.

Secondary metabolites have a wide variety of biological functions to aid the host organism, which includes their highly exploited antimicrobial activity, hormone-like regulation of differentiation, quorum sensing, roles in metal transport, and diffusible siderophores (Challis and Hopwood, 2003; Linares et al., 2006). Of interest to us are those that possess antimicrobial activity. Antibiotics are one of the most successful classes of drugs that have been used in the clinic. However, their extensive use in medicine and agriculture has imposed an immense selective pressure for resistant isolates

to emerge. During the ‘Golden Age’ of antibiotic discovery in the 1950s, most of the known classes of antibiotic were isolated as natural products from actinomycetes. This constituted the ‘low hanging fruit’ of natural products as termed by Richard Baltz (Baltz, 2005), where compounds that were easy to isolate in the laboratory were discovered. However, it has since been challenging to identify new classes of antibiotics as natural products. Therefore, we must seek other means in order to increase the chemical diversity that is available to us.

1.4. Project Objectives

In order to combat ever evolving antibiotic resistance mechanisms, we must constantly seek new antibiotics. To do so, we require access to a greater variety of chemicals that are currently available to us. There are several ways to increase our chemical repertoire. One approach would be to search the soil for new antibiotics. This can be done by either sampling rare actinomycetes that were previously avoided due to difficulties in culturing them in the laboratory, or by trying to identify ways of making the well known antibiotic producing actinomycetes to produce different secondary metabolites. It is well known that actinomycetes can produce a large variety of secondary metabolites (Bentley et al., 2002), however in the laboratory it is often difficult to provide appropriate conditions for these organism to produce their whole array of compounds. Thus, we must seek growth conditions that will allow actinomycetes to produce secondary metabolites that have been overlooked in the past. Another approach to

increase chemical diversity would be to chemically synthesize novel antibiotic scaffolds. However, to reproduce the chemical complexity of natural products in the laboratory can be challenging, expensive, inefficient, and labour intensive, which makes this approach unattractive. A third approach and one that we are interested in is to utilize the machinery that constructs natural products to modify pre-existing compounds. By modifying secondary metabolite biosynthetic pathways, we can engineer compounds that would be more favourable for chemical modification and would thus allow us to produce semi-synthetic compounds. Using this method in accordance with knowledge of drug-target binding information, we can rationally design antibiotics that maintain their biological activity while evading resistance mechanisms.

Therefore, our objectives are to increase chemical diversity by constructing semi-synthetic natural products. However, to do so we must gain a deeper understanding of the biosynthetic mechanisms used to assemble natural products. Methyltransferases are a group of enzymes that are commonly found in secondary metabolite biosynthetic pathways. Our intentions are to utilize methyltransferases as agents to increase chemical diversity.

1.5. Methyltransferases

Methylation reactions are vital to many cellular processes both in prokaryotic and eukaryotic organisms. The transfer of a methyl group is catalyzed by methyltransferase enzymes and not surprisingly a vast number of methyltransferases have been identified and studied (Martin and McMillan, 2002). These enzymes can use several types of

substrates as methyl donors including folate coenzymes such as N^5 -methyl-tetrahydrofolate, methyl-Coenzyme B₁₂, and S-adenosylmethionine (SAM) (Walsh, 1979). However, SAM is by far the most common substrate for methyltransferases and SAM-dependent methyltransferases are the most abundant enzymes encountered in natural product biosynthesis (Martin and McMillan, 2002). SAM-dependent methyltransferases have been known to catalyze the methylation of a vast array of substrates including small molecules, DNA, RNA, proteins, polysaccharides, and lipids (Cheng and Roberts, 2001). Figure 1.3 illustrates a typical methyltransferase reaction where the enzyme methylates a substrate by using SAM and converting it to S-adenosyl-L-homocysteine (SAH). Enzymatic reactions are believed to proceed through a nucleophilic attack of a lone pair of electrons on either a sulphur, oxygen, or a nitrogen atom on the methyl group of SAM (Walsh, 1979).

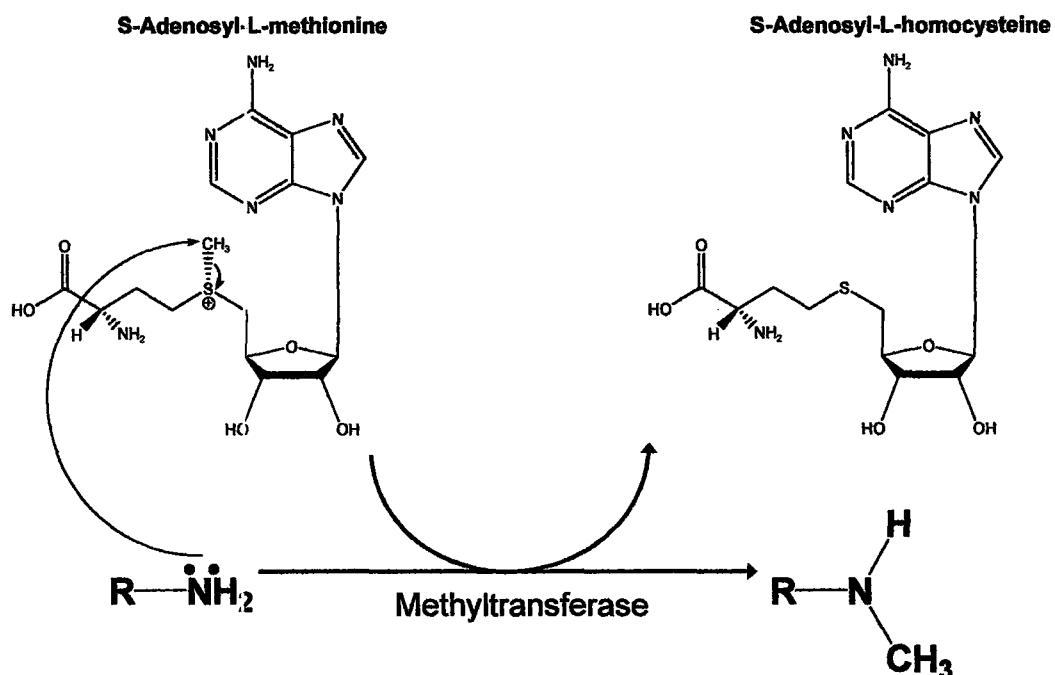


Figure 1.3. A typical methyltransferase reaction mechanism where the enzyme catalyzes the methylation of a substrate by utilizing S-adenosyl-L-methionine and converting it to S-adenosyl-L-homocysteine. Reaction proceeds through a nucleophilic attack of a lone pair of electrons from the nitrogen atom on the methyl group of S-adenosyl-L-methionine.

The core SAM-dependent methyltransferase fold is composed of a SAM binding region in the N-terminus and a substrate binding region in the C-terminus. The core fold is composed of seven β strands in the general order of 3214576 separated by six α helices (Martin and McMillan, 2002). Despite a highly conserved core fold, there is little conservation of amino acid residues that interact with SAM (Loenen, 2006). In general, SAM binds different methyltransferases in a similar fashion but the detailed chemistry of interaction between the substrate and the protein is different among enzymes (Martin and

McMillan, 2002). As expected, there is great diversity in the structure of the C-terminal substrate binding region of SAM-dependent methyltransferases. This is due to the ability of these enzymes to bind a large variety of substrates differing in size, shape, and chemistry (Martin and McMillan, 2002).

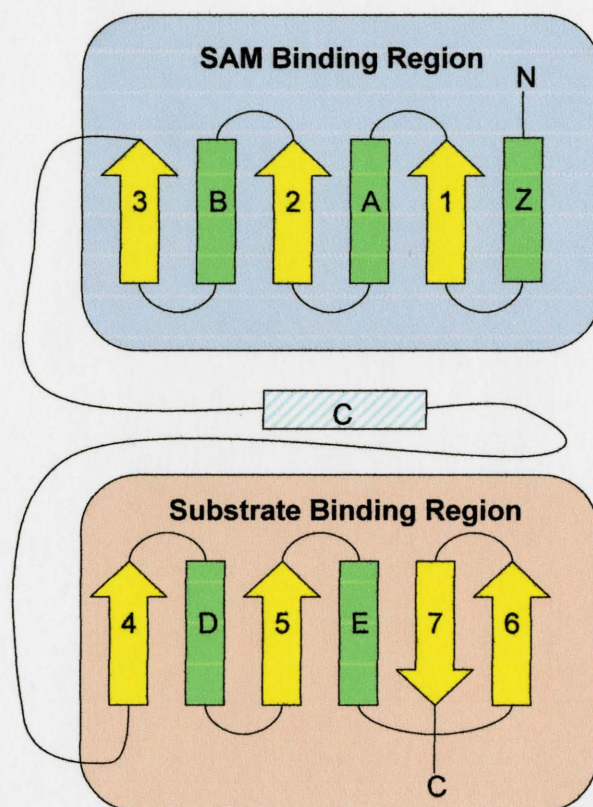


Figure 1.4. The core fold of SAM-dependent methyltransferases. The core fold is composed of seven β strands numbered 1-7 (yellow arrows) and six α helices labelled A-E and Z (green rectangles). Helix C is shown separately because it may not always be present in the core fold. This figure was adapted from Martin and McMillan, 2002 (Martin and McMillan, 2002).

Methylation reactions are present in many secondary metabolite biosynthetic pathways, and thus they can be exploited to increase chemical diversity. However, before we can use these enzymes to modify compounds, we must gain a deeper understanding of their biochemistry. By performing *in vitro* studies on SAM-dependent methyltransferases that participate in natural product biosynthesis, we will be able to better assess their potential. Herein, we investigate two SAM-dependent methyltransferases. One enzyme, OxyT, is believed to be a putative SAM-dependent methyltransferase that methylates an oxytetracycline intermediate (Zhang et al., 2006). This enzyme has never been studied and its characterization would allow us to better understand oxytetracycline biosynthesis. The second enzyme, MtfA, was discovered in the chloroeremomycin biosynthetic cluster and has been shown to methylate other glycopeptide scaffolds (van Wageningen et al., 1998; O'Brien et al., 2000). We have previously shown that this enzyme is active *in vivo* (Lamb, 2007), and intent to characterize it *in vitro*.

Reference List

Baltz,R.H. (2005). Antibiotic discovery from actinomycetes: Will a renaissance follow the decline and fall? *SIM News* 55, 186-196.

Bentley,S.D., Chater,K.F., Cerdeno-Tarraga,A.M., Challis,G.L., Thomson,N.R., James,K.D., Harris,D.E., Quail,M.A., Kieser,H., Harper,D., Bateman,A., Brown,S., Chandra,G., Chen,C.W., Collins,M., Cronin,A., Fraser,A., Goble,A., Hidalgo,J., Hornsby,T., Howarth,S., Huang,C.H., Kieser,T., Larke,L., Murphy,L., Oliver,K., O'Neil,S., Rabbinowitsch,E., Rajandream,M.A., Rutherford,K., Rutter,S., Seeger,K., Saunders,D., Sharp,S., Squares,R., Squares,S., Taylor,K., Warren,T., Wietzorrek,A., Woodward,J., Barrell,B.G., Parkhill,J., and Hopwood,D.A. (2002). Complete genome sequence of the model actinomycete *Streptomyces coelicolor* A3(2). *Nature* 417, 141-147.

Berdy,J. (2005). Bioactive microbial metabolites. *J. Antibiot. (Tokyo)* 58, 1-26.

Challis,G.L. and Hopwood,D.A. (2003). Synergy and contingency as driving forces for the evolution of multiple secondary metabolite production by *Streptomyces* species. *Proc. Natl. Acad. Sci. U. S. A* 100 *Suppl* 2, 14555-14561.

Chater,K.F. (2006). *Streptomyces* inside-out: a new perspective on the bacteria that provide us with antibiotics. *Philos. Trans. R. Soc. Lond B Biol. Sci.* 361, 761-768.

Chater,K.F. (1993). Genetics of differentiation in *Streptomyces*. *Annu. Rev. Microbiol.* 47, 685-713.

Cheng,X. and Roberts,R.J. (2001). AdoMet-dependent methylation, DNA methyltransferases and base flipping. *Nucleic Acids Res.* 29, 3784-3795.

Hopwood,D.A. (2007). *Streptomyces* in Nature and Medicine: The Antibiotic Makers. (Toronto: Oxford University Press).

Huxley,T.H. (1869). Nature: Aphorisms by Goethe. *Nature* 1, 9-11.

Lai,J.R., Koglin,A., and Walsh,C.T. (2006). Carrier protein structure and recognition in polyketide and nonribosomal peptide biosynthesis. *Biochemistry* 45, 14869-14879.

Lamb, S. S. Glycopeptide Antibiotics: Sulfation and Modification. 121-162. 2007. McMaster University, McMaster University.
Ref Type: Thesis/Dissertation

Linares, J.F., Gustafsson, I., Baquero, F., and Martinez, J.L. (2006). Antibiotics as intermicrobial signaling agents instead of weapons. *Proc. Natl. Acad. Sci. U. S. A* *103*, 19484-19489.

Loenen, W.A. (2006). S-adenosylmethionine: jack of all trades and master of everything? *Biochem. Soc. Trans.* *34*, 330-333.

Martin, J.L. and McMillan, F.M. (2002). SAM (dependent) I AM: the S-adenosylmethionine-dependent methyltransferase fold. *Curr. Opin. Struct. Biol.* *12*, 783-793.

O'Brien, D.P., Kirkpatrick, P.N., O'Brien, S.W., Staroske, T., Richardson, T.I., Evans, D.A., Hopkinson, A., Spencer, J.B., and Williams, D.H. (2000). Expression and assay of an N-methyltransferase involved in the biosynthesis of a vancomycin group antibiotic. *Chem. Comm.* 103-104.

Ohnishi, Y., Ishikawa, J., Hara, H., Suzuki, H., Ikenoya, M., Ikeda, H., Yamashita, A., Hattori, M., and Horinouchi, S. (2008). Genome sequence of the streptomycin-producing microorganism *Streptomyces griseus* IFO 13350. *J. Bacteriol.* *190*, 4050-4060.

Oliynyk, M., Samborsky, M., Lester, J.B., Mironenko, T., Scott, N., Dickens, S., Haydock, S.F., and Leadlay, P.F. (2007). Complete genome sequence of the erythromycin-producing bacterium *Saccharopolyspora erythraea* NRRL23338. *Nat. Biotechnol.* *25*, 447-453.

van Wageningen, A.M.A., Kirkpatrick, P.N., Williams, D.H., Harris, B.R., Kershaw, J.K., Lennard, N.J., Jones, S.J.M., and Solenberg, P.J. (1998). Sequencing and analysis of genes involved in the biosynthesis of a vancomycin group antibiotic. *Chemistry and Biology* *5*, 155-162.

Walsh, C. (1979). *Enzymatic Reaction Mechanisms*. (San Francisco: W. H. Freeman and Company).

Zakeri, B. and Wright, G.D. (2008). Chemical biology of tetracycline antibiotics. *Biochem. Cell Biol.* *86*, 124-136.

Zhang, W., Ames, B.D., Tsai, S.C., and Tang, Y. (2006). Engineered biosynthesis of a novel amidated polyketide, using the malonamyl-specific initiation module from the oxytetracycline polyketide synthase. *Appl. Environ. Microbiol.* *72*, 2573-2580.

**CHAPTER 2: INVESTIGATION OF A TETRACYCLINE
METHYLTRANSFERASE**

Chapter 2: Investigation of A Tetracycline Methyltransferase

2.1. Introduction

Tetracyclines were first introduced into the clinic in the 1950's and have since been a very successful class of antibiotics. These compounds are broad spectrum antibiotics with activity against a plethora of microbes from diverse physiological, ecological, and genetic backgrounds (Zakeri and Wright, 2008). As a result, they are among the drugs of choice for first line defence against an unknown infection. Compounded by the fact that they are naturally produced by *Streptomyces* bacteria and thus can be cost-effectively isolated from fermentation broths, they have been an attractive group of antibiotics for the pharmaceutical industry (Zakeri and Wright, 2008; Chopra and Roberts, 2001).

Tetracyclines are bacteriostatic antimicrobials that function by inhibiting bacterial protein translation. They do so by binding to the 30S ribosomal subunit near the A-site and subsequently inhibiting aminoacylated-tRNA from docking (Brodersen et al., 2000; Pioletti et al., 2001). In order to combat these effects, bacteria possess several forms of resistance mechanisms. The most clinically relevant resistance mechanisms are energy-dependent drug efflux and ribosomal protection proteins that bind the ribosome, thereby inhibiting tetracycline from binding (Burdett, 1991; Zakeri and Wright, 2008). Other reported resistance mechanisms that are not yet of significant clinical importance include

drug modification by a monooxygenase (Yang et al., 2004) and target alteration through a mutation in 16S rRNA (Ross et al., 1998).

A well studied member of the tetracyclines is oxytetracycline, which is produced by *Streptomyces rimosus*. Oxytetracycline biosynthesis has been studied since the early 1960's, yet it has only been recently that we have attained a deeper understanding of the biosynthetic process. Tetracyclines belong to the polyketide class of natural products and are produced by Type II polyketide synthases (PKS). Unlike Type I PKSs and nonribosomal peptide synthetases (NRPS) that are single mega-enzyme complexes containing many distinct modules responsible for increasing the nascent polyketide or peptide chain respectively, Type II PKSs function as separate subunits (Lai et al., 2006). Consequently, many distinct enzymes perform the tailoring reactions that form the richly decorated polyketide compounds and in the process these enzymes produce highly unstable intermediates. The disseminated nature of this biosynthetic mechanism and the challenges of isolating reaction intermediates has lead to many difficulties in studying this process which is still poorly understood (Hertweck et al., 2007; Zakeri and Wright, 2008).

One such tailoring enzyme present in the oxytetracycline biosynthetic pathway is the putative methyltransferase OxyT. It is believed that OxyT is responsible for catalyzing the dimethylation of 4-amino-anhydrotetracycline to anhydrotetracycline using two molar equivalents of SAM (Figure 2.1). Although tetracycline biosynthesis has been studied through blocked mutant analysis, substrate feeding experiments, and precursor analysis, to our knowledge biochemical characterization of tailoring enzymes has never

been reported. Furthermore, for future studies our laboratory is interested in producing an *oxyT* deficient mutant of *S. rimosus*, which we believe would produce the precursor compound 4-amino-anhydrotetracycline that would serve as a scaffold for constructing novel tetracycline derivatives. Previous studies have established that the keto-enol functionalities on the hydrophilic region of tetracyclines are essential for activity and make key contacts to the 16S RNA component of the 30S ribosomal subunit in the tetracycline binding site (Figure 2.2) (Brodersen et al., 2000; Pioletti et al., 2001; Zakeri and Wright, 2008). However, the more hydrophobic region of tetracyclines has been shown to be more tolerant of modifications and indeed most of the chemical diversity seen among tetracyclines occurs in this region. In fact, based on the crystal structure of tetracycline in complex with the 30S ribosomal subunit, we can see the more hydrophobic region of the molecule appears to be in open space and does not make contacts with the ribosome (Figure 2.2) (Zakeri and Wright, 2008). Also, it has previously been demonstrated that the C4 dimethylamino moiety of tetracycline makes key contacts to TetR, a transcriptional regulatory protein that controls the expression of the commonly found tetracycline efflux pump, TetA (Hinrichs et al., 1994). Yet, modifications at the C4 dimethylamino moiety of tetracyclines have not been thoroughly investigated. We believe the C4 dimethylamino moiety of tetracyclines can serve as an entry point for the construction of novel tetracyclines. However, prior to these studies we first intend to biochemically characterize OxyT to prove that it is in fact responsible for the dimethylation of 4-amino-anhydrotetracycline.

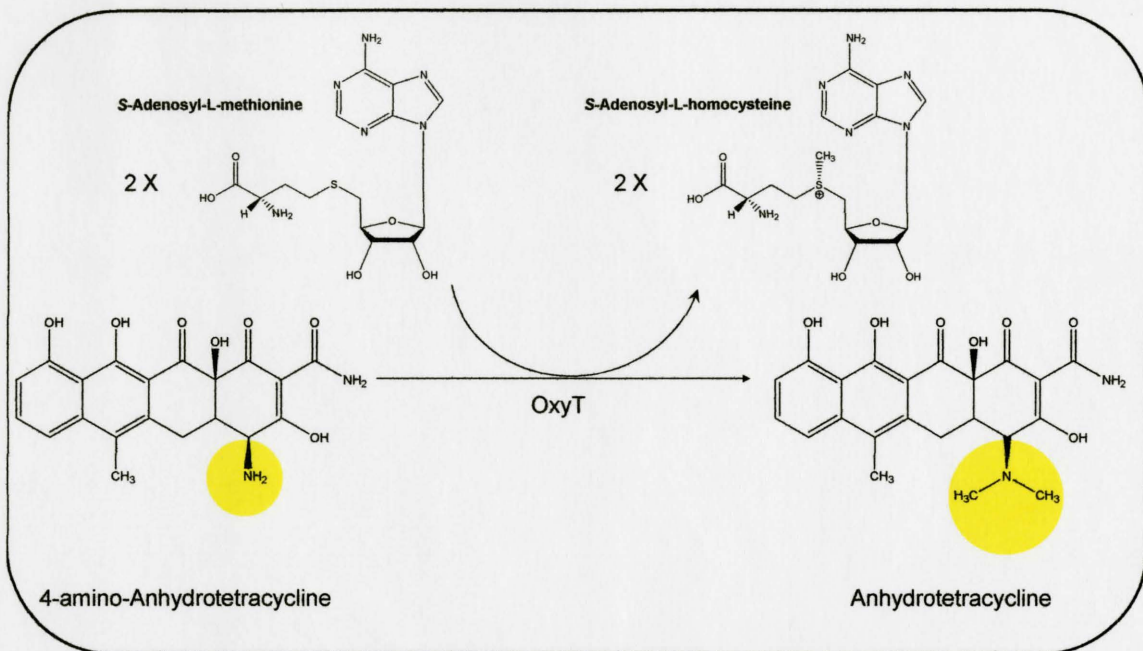


Figure 2.1. The dimethylation reaction catalyzed by OxyT. OxyT is a putative methyltransferase that is believed to dimethylate 4-amino-anhydrotetracycline to produce anhydrotetracycline using two molar equivalents of S-adenosyl-L-methionine.

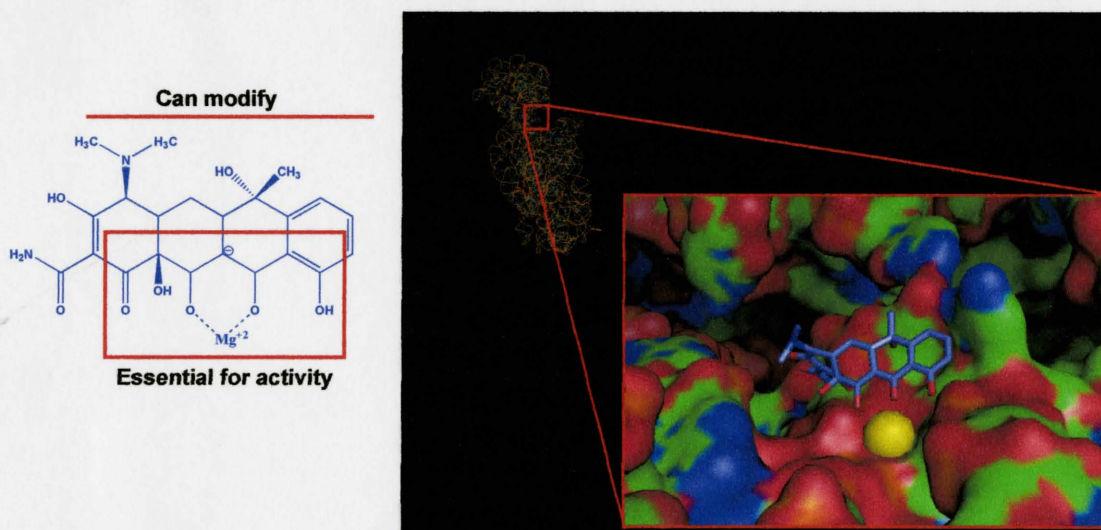


Figure 2.2. Tetracycline binding to the 30S ribosomal subunit. The left panel shows the chemical structure of tetracycline in complex with Mg²⁺. The boxed region on the hydrophilic side of the molecule is required for binding to the 30S ribosomal subunit

(right panel) where it makes key contacts to 16S RNA. However, the more hydrophobic region of the molecule appears to be in open space and is more tolerant to modification (Zakeri and Wright, 2008). PDB file 1I97.

2.2. Materials and Methods

2.2.1. Cloning of the *oxyT* gene

The *oxyT* gene was cloned into the pDEST17 expression vector containing an N-terminal 6X His tag using Gateway[®] Technology as per manufacturers instructions (Invitrogen, 2003). To amplify *oxyT*, the following primers were used: forward primer 5' – GGGGACAAGTTTGTACAAAAAAGCAGGCTTCGAAAACCTGTATTTTCAG GGCAGTCCCATGACCACCACAC – 3' and reverse primer 5' – GGGGACCACTT TGTACAAGAAAGCTGGGTCGGCATGATCACGGTAGCA – 3'. *S. rimosus* (ATCC 10970) genomic DNA was used as a template for PCR amplification, and it was isolated by growing a 25 mL culture (in a 50 mL Erlenmeyer flask) of *S. rimosus* in TSB medium (Per 500 mL: 15 g of Oxoid tryptone soya broth powder (CM129)) containing an ~2 cm spring for aeration and incubated at 30°C for 3 days at 250 rpm. The culture was centrifuged at 3000 rpm for 10 min on a Sorvall RT 6000B centrifuge, then re-suspended in 10 mL SET buffer (20 mM Tris pH 7.5, 75 mM NaCl, and 25 mM EDTA pH 8.0) and homogenized in a glass homogenizer. Pellets were washed again in SET buffer, then re-suspended in 5 mL SET buffer and 200 µL of lysozyme (50 mg/mL) was added and the sample was incubated at 37°C for 60 min. Subsequently, 140 µL of proteinase K (20 mg/mL) and 600 µL of 20% SDS was added and the sample was incubated at 55°C for 2 hours, inverting occasionally. Once the sample had cooled down, 2 mL of 5 M NaCl was

added, mixed and then 10 mL of chloroform was added and the sample was incubated at room temperature for 30 min on a rocker. The sample was then centrifuged at 4500g for 15 min on a Beckman Coulter Avanti™ J-25 centrifuge and genomic DNA was precipitated by adding 0.6 volumes of isopropanol to the aqueous phase. The DNA was rinsed in 5 mL of 70% ethanol and air dried. Finally, the genomic DNA was re-suspended in 1 mL TE buffer (10 mM Tris and 1 mM EDTA at pH 8.0). To amplify the *oxyT* gene, the following 25 μ L polymerase chain reaction (PCR) was setup: 1 mM dNTPs, 0.5 μ L *S. rimosus* genomic DNA, 2 μ M of each primer, 5% DMSO, 10 mM MgCl₂, and 0.5 U Biotools DNA polymerase. The following PCR program was used to amplify *oxyT*: 94°C for 3 min, 30 cycles of (94°C for 1 min, 49.5°C for 1 min, 72°C for 1 min), and 72°C for 10 min.

Briefly, based on the Gateway® Technology protocol (Invitrogen, 2003), *oxyT* was first cloned into pDONR201 by setting up the following BP reaction: 3 μ L PCR product, 1 μ L pDONR201 vector, 2 μ L 5X BP Clonase Reaction Buffer, 2 μ L TE buffer (pH 8.0), and 2 μ L BP Clonase Enzyme Mix. The reaction was incubated at room temperature for 2.5 hours and 2 μ L of Proteinase K (2 μ g/mL) was added and further incubated at 37°C for 10 min. The reaction was transformed into *Escherichia coli* TOP10 using electroporation and plated on Luria-Bertani (LB) media (50 μ g/mL kanamycin). Colonies were screened by PCR analysis and complete gene sequencing. To sub-clone *oxyT* from pDONR201 into the expression vector pDEST17, the following LR reaction was setup: 2 μ L pDONR201-*oxyT*, 1 μ L pDEST17 vector, 2 μ L 5X LR Clonase Reaction Buffer, 5 μ L TE buffer (pH 8.0), and 2 μ L LR Clonase Enzyme Mix. The reaction was

incubated at room temperature for 3 hours, then 2 μ L of Proteinase K (2 μ g/mL) was added and further incubated at 37°C for 10 min. The reaction was transformed into *E. coli* TOP10 using electroporation and plated on LB media (100 μ g/mL ampicillin). Colonies were screened by restriction digestion analysis and complete gene sequencing.

2.2.2. Expression and Purification of OxyT

The *oxyT* gene cloned into the expression vector pDEST17 containing an N-terminal 6X His tag, was transformed in to *E. coli* Rosetta Gami pLysS cells using electroporation. These constructs were grown overnight in LB media (100 μ g/mL ampicillin and 25 μ g/mL chloramphenicol). 10 mL of an overnight culture was used to inoculate 1 L of LB media (100 μ g/mL ampicillin and 25 μ g/mL chloramphenicol) and cultures were growth at 37°C and 250 rpm until an OD₆₀₀ of ~0.6. Subsequently, IPTG (0.1 mM final concentration) was added to the cultures and they were grown overnight at 16°C and 240 rpm. Cultures were centrifuged (5000g for 20 min on a Beckman Coulter Avanti™ J-25 centrifuge), then pellets were re-suspended in 20 mL 0.85% (w/v) saline and centrifuged again (3000 rpm for 20 min) and pellets were stored at -80°C.

Cell pellets were lysed using a French Press (American Instrument Company), lysates were centrifuged at 18000 rpm for 30 min at 4°C and supernatants were immediately applied to a Ni-NTA column with a ~2 mL bed volume (Qiagen Canada). Lysates were washed with 50 mM NaH₂PO₄ and 300 mM NaCl buffer pH 8.0 with increasing amounts of imidazole (10 mM, 20 mM, and 50 mM), and protein was eluted with 250 mM imidazole. Protein fractions were analyzed by running on a 15% SDS-polyacrylamide gel and protein containing fractions were pooled and dialyzed against 50

mM HEPES pH 7.5 and 5 mM MgCl₂ (for initial experiments) or 50 mM NaH₂PO₄ pH 7.5 (for later experiments). Protein concentration was determined using a Bradford assay (reagent from Bio-Rad Laboratories).

2.2.3. OxyT Activity Assays

OxyT activity was tested against three commercially available compounds ((*R*)-(-)-1,2,3,4-tetrahydro-1-naphthylamine, 1-naphthylamine, and 1-aminoanthracene) since its predicted natural substrate (4-amino-anhydrotetracycline) was not available. Initial experiments to test for OxyT activity were followed by reverse phase-high performance liquid chromatography (RP-HPLC). The enzymatic reactions were prepared as follows: 100 µM substrate, 100 µM SAM, 0.1 µg OxyT in 50 mM HEPES buffer at pH 7.5 (incubate at 30°C overnight). Reaction progress was analyzed by RP-HPLC (DIONEX GP40 HPLC) on a Grace Vydac #126 C18 column with solvent A containing H₂O with 0.05% trifluoroacetic acid and solvent B containing acetonitrile with 0.05% trifluoroacetic acid (Program: 0-1 min 95% A and 5% B, 11 min 3% A and 97% B, 12.5 min 95% A and 5% B, 14.1 min 95% A and 5% B). Further assays were performed with OxyT and higher reagent concentration and analyzed by liquid chromatography/mass spectrometry (LC/MS). The enzymatic reactions were prepared as follows: 1.0 mM substrate, 1.0 mM SAM, 1.0 µg OxyT in 50mM HEPES buffer at pH7.5 (incubate at 30°C for 5 days). For LC/MS (Agilent 1100 Series HPLC, Applied Biosystems QTRAP LC/MS/MS, Analyst Software 4.0) analysis, samples were run through a Grace Vydac #126 C18 column with solvent A containing H₂O with 0.05% formic acid and solvent B

containing acetonitrile with 0.05% formic acid (Program: 0-1 min 95% A and 5% B, 11 min 3% A and 97% B, 12.5 min 95% A and 5% B, 14.1 min 95% A and 5% B).

2.2.4. Analytical Gel Filtration of OxyT

OxyT was analyzed by gel filtration on an AmershamPharmaciaBiotech ÄKTA FPLC UPC-900 using a Superdex 200 HR 10/30 gel filtration column and analyzing data with Unicorn 4.12 software. OxyT was stored in 50 mM NaH₂PO₄ buffer pH 8.0 with 5% glycerol at a concentration of 1.2 mg/mL, and the running buffer used contained 50 mM NaH₂PO₄ buffer pH 8.0 and 200 mM NaCl. To load columns, 200 µL of sample was injected onto the column at a flow rate of 0.2 mL/min for 3 injection volumes and subsequently the flow rate was adjusted to 0.5 mL/min.

2.3. Results and Discussion

Biochemical characterization of tailoring enzymes in type II PKS biosynthetic pathways have been challenging due to difficulties in isolation of the natural substrate for the respective enzymes (Hertweck et al., 2007; Zakeri and Wright, 2008). Tetracycline modifying enzymes are no exception to this fact. Consequently, we intended to study the putative methyltransferase OxyT to gain a deeper insight into tetracycline biosynthesis and to aid future studies for the design of novel tetracyclines. Without the availability of 4-amino-anhydrotetracycline, OxyT's predicted natural substrate, we decided to test whether OxyT would demonstrate methyltransferase activity on commercially available compounds that resemble 4-amino-anhydrotetracycline (Figure 2.1). Therefore, we tested OxyT methyltransferase activity on (R)-(-)-1,2,3,4-tetrahydro-1-naphthylamine, 1-naphthylamine, and 1-aminoanthracene (Figure 2.3).

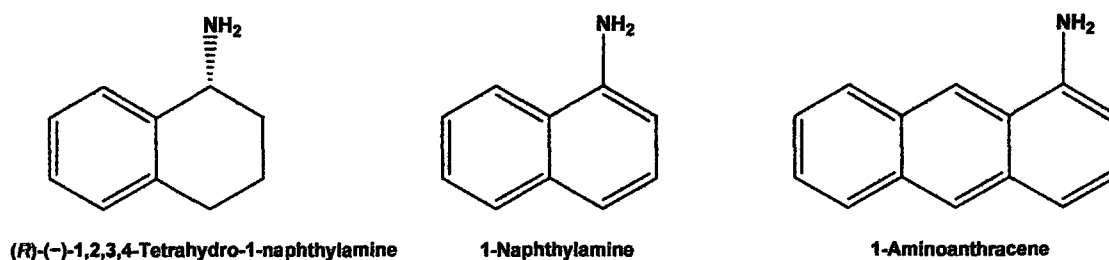
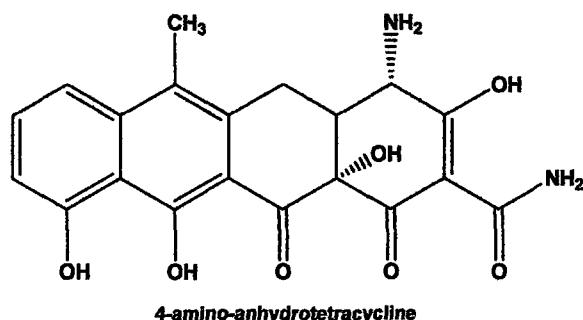


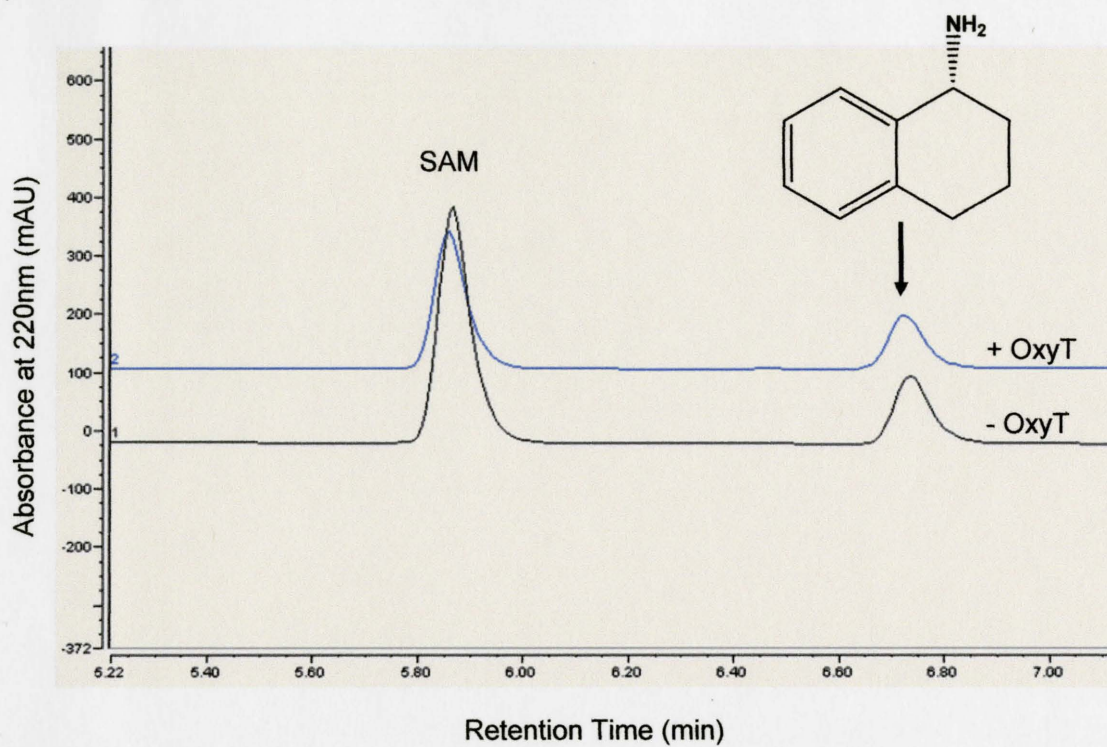
Figure 2.3. Compounds used to test OxyT activity.

The *oxyT* gene was cloned into a pDEST17 expression vector containing an N-terminal 6X His tag. Initial solubility tests showed that OxyT was insoluble when expressed in *E. coli* BL21(DE3) cells but it was partially soluble when expressed in *E. coli* Rosetta Gami pLysS cells. Therefore, *oxyT* was expressed in *E. coli* Rosetta Gami pLysS cells and purified using a Ni-NTA column.

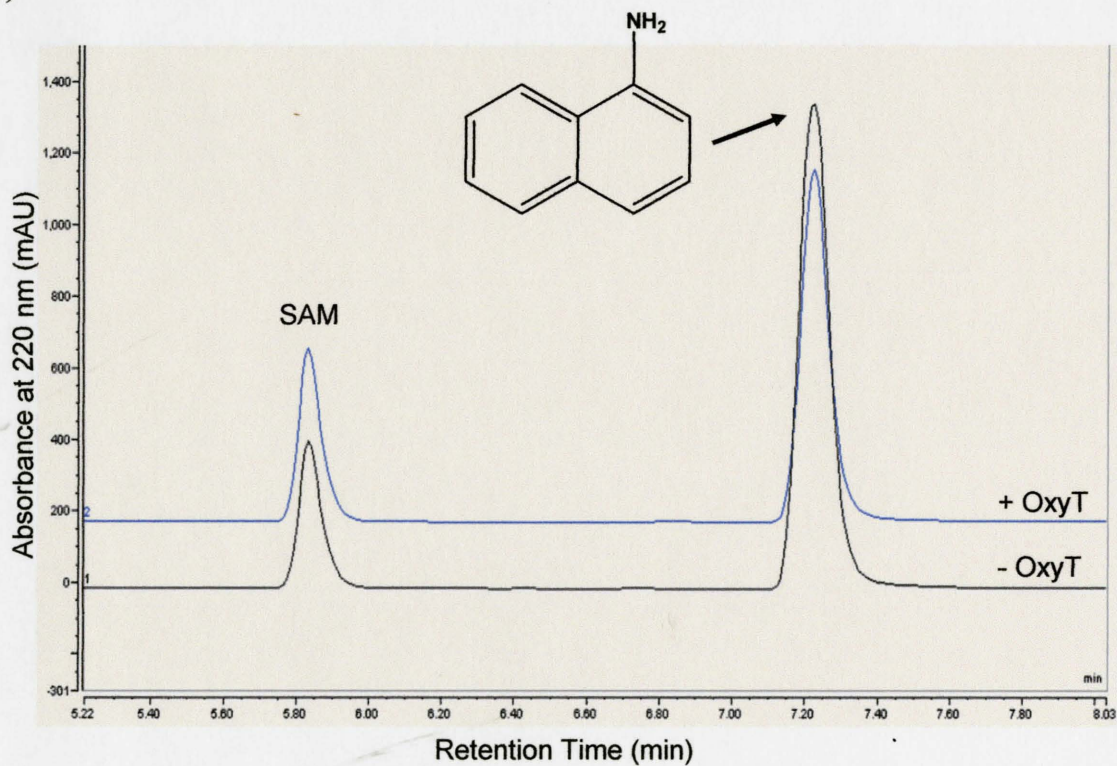
OxyT activity was tested against the three putative substrates (R)-(-)-1,2,3,4-tetrahydro-1-naphthylamine, 1-naphthylamine, and 1-aminoanthracene by performing the following enzymatic reaction: 50 mM HEPES pH 7.5, 100 μ M substrate, 100 μ M SAM, and 0.1 μ g OxyT. Reactions were incubated overnight at 30°C and due to a lack of an

appropriate assay, reaction progress was detected by RP-HPLC (Figure 2.4). Methylation of the putative substrates (R)-(-)-1,2,3,4-tetrahydro-1-naphthylamine, 1-naphthylamine, and 1-aminoanthracene was not detected. To ensure that the observed lack of activity was not due to an inability to detect the methylated product by RP-HPLC, we decided to test activity on LC/MS at ten fold higher concentrations. Thus, the following reactions were tested: 50 mM HEPES pH 7.5, 1.0 mM substrate, 1.0 mM SAM, and 1.0 μ g OxyT. The reactions were incubated for 5 days at 30°C and analyzed by LC/MS (Figure 2.5). However, even at higher reaction concentrations and a longer incubation time, methylation of the substrates was not detected. An addition of a single methyl group would increase the molecular weight by 14 and dimethylation would increase the molecular weight by 28, but these mass increases were not observed for any of the putative substrates (Figure 2.5).

a)



b)



c)

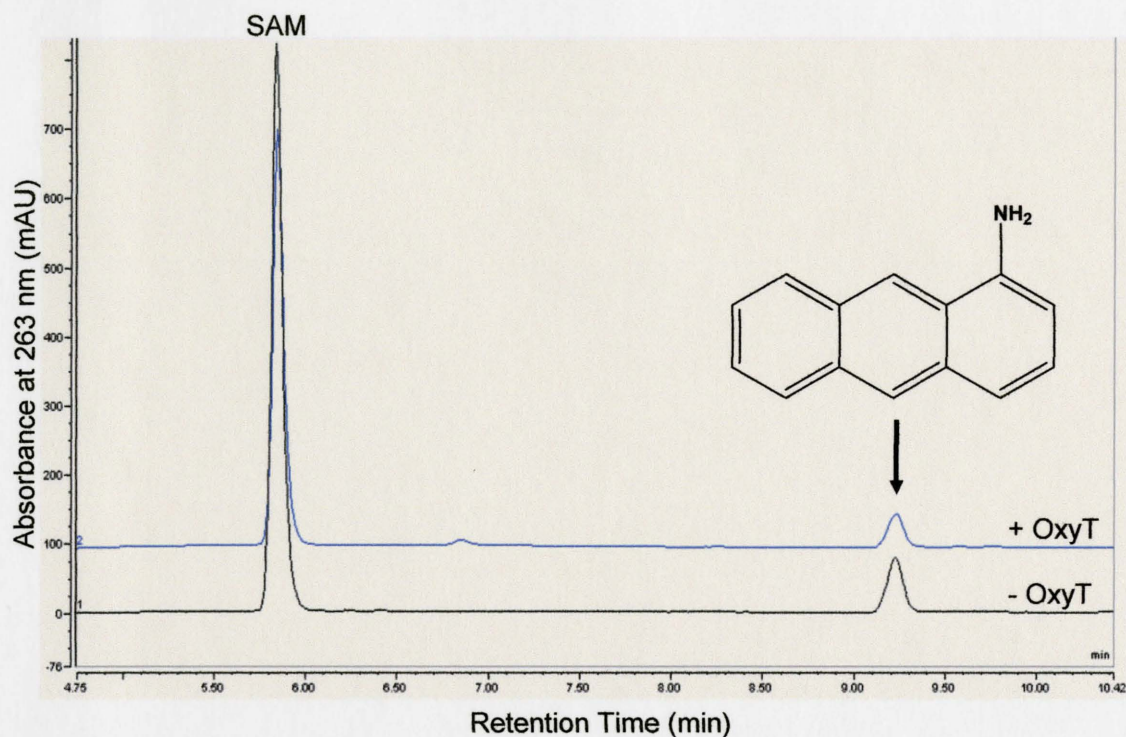


Figure 2.4. OxyT enzymatic assays. OxyT enzymatic activity was tested on (a) (R)-(-)-1,2,3,4-tetrahydro-1-naphthylamine, (b) 1-naphthylamine, and (c) 1-aminoanthracene by the following reaction conditions: 50 mM HEPES pH 7.5, 100 μ M substrate, 100 μ M SAM, and 0.1 μ g OxyT (incubate overnight at 30°C). Reactions were analyzed by RP-HPLC using a Grace Vydac #126 C18 column.

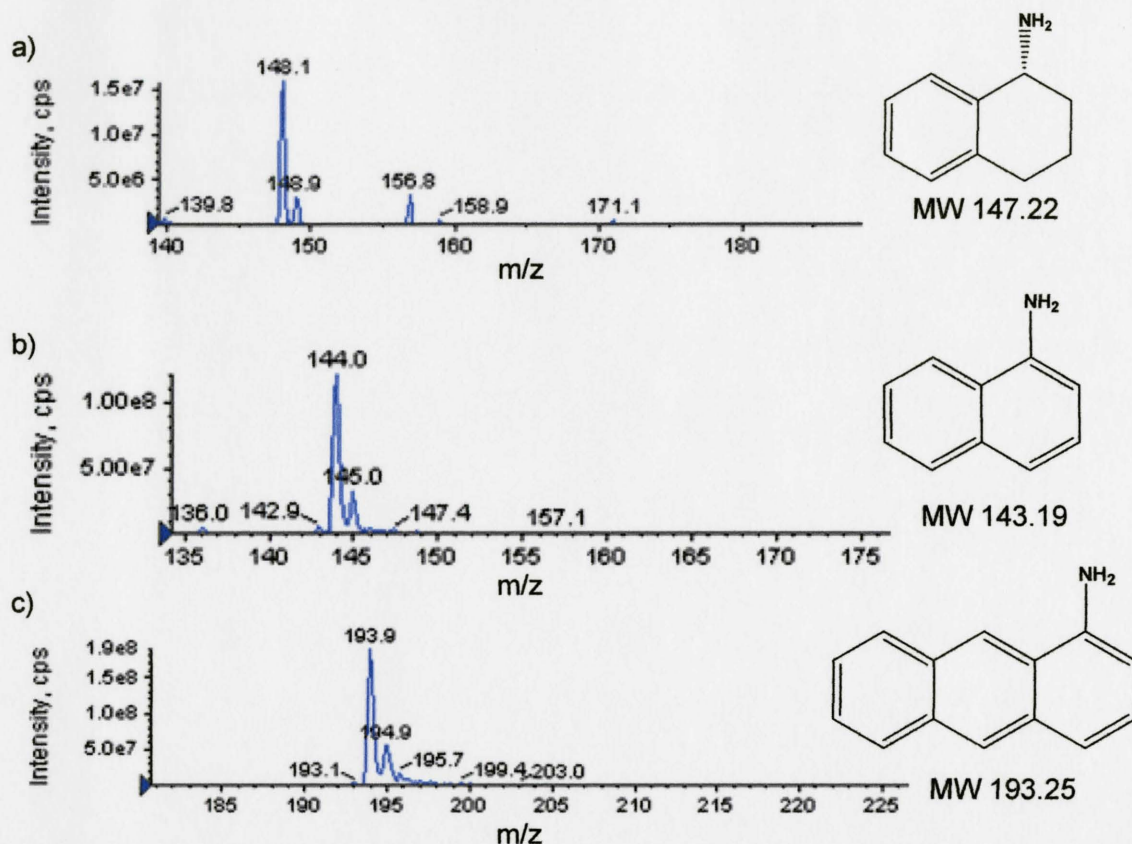


Figure 2.5. OxyT enzymatic assays analyzed by LC/MS. OxyT enzymatic activity was tested on (a) (R)-(-)-1,2,3,4-tetrahydro-1-naphthylamine, (b) 1-naphthylamine, and (c) 1-aminoanthracene by the following reaction conditions: 50 mM HEPES pH 7.5, 1.0 mM substrate, 1.0 mM SAM, and 1.0 μ g OxyT (incubate for 5 days at 30°C). Reactions were analyzed by LC/MS using a Grace Vydac #126 C18 column RP-HPLC column.

OxyT was further analyzed by gel filtration to decipher whether the protein is present as a monomer or a homodimer, since many small molecule methyltransferases are homodimers. However, rather than producing a single peak on the gel filtration run, the OxyT peak was very broad with many small crescents (Figure 2.6). This may be due to a mis-folded protein and would be consistent with our activity assays. Therefore, the lack of observed activity for OxyT may be due to a mis-folded protein or that the compounds

tested are not appropriate substrates for OxyT. Thus, we decided that the ideal way to analyze OxyT would be to test its activity on its predicted natural substrate. In order to obtain the predicted natural substrate for OxyT and a tetracycline scaffold that may be used to construct novel tetracyclines, we decided to disrupt the *oxyT* gene in *S. rimosus*.

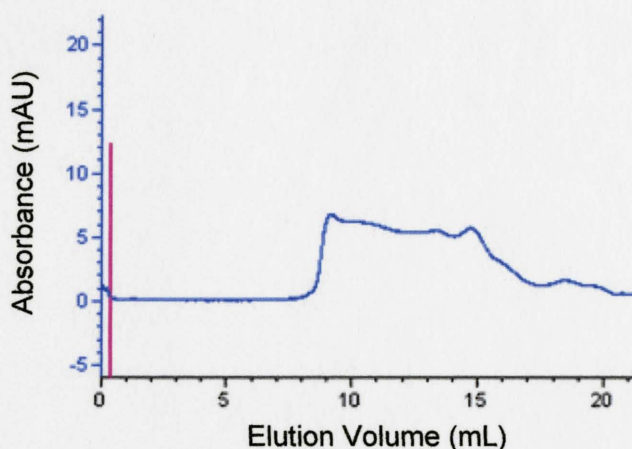


Figure 2.6. Gel filtration analysis of OxyT. OxyT was loaded onto a Superdex 200 HR 10/30 gel filtration column at a concentration of 1.2 mg/mL on a AmershamPharmaciaBiotech ÄKTA FPLC UPC-900 system. The line at 0.2 mL represents the point of sample injection.

In order to disrupt the *oxyT* gene, we attempted to insert an antibiotic resistance marker in the middle of the gene (methods and results are outlined in the Appendix). In our experiments we obtained antibiotic resistant mutants of *S. rimosus*, but our screens demonstrated that these mutants possessed an intact *oxyT* gene. Therefore, we were unable to successfully isolated *S. rimosus* Δ *oxyT* mutants.

2.4. Conclusions

Tetracyclines are broad spectrum antibiotics that have been clinically used to fight bacterial infections for over half a century. However, the emergence of resistant pathogens has severely limited the use of these antibiotics. In order to rationally design novel tetracycline derivatives, we must first gain a deeper understanding of the biosynthetic pathways that produce these compounds. By achieving a better understanding of the tailoring enzymes that modify tetracycline scaffolds, we may be able to use the catalytic efficiency of enzymes to construct semi-synthetic compounds that maintain biological activity but can evade resistance mechanisms. Herein, we attempted to characterize OxyT, a putative tetracycline N-methyltransferase.

Due to a lack of OxyT's predicted natural substrate, we tested OxyT activity against similar commercially available compounds, but we were unable to detect methylation of these compounds. Therefore, we decided to isolate OxyT's predicted natural substrate by constructing an *oxyT*-null *S. rimosus* mutant, but we were unsuccessful. In our future studies, we intend to construct an *S. rimosus* $\Delta oxyT$ mutant by constructing a plasmid that contains an antibiotic selection marker situated in between ~1 kb sequences of DNA that corresponds to sequences flanking *oxyT* in the *S. rimosus* genome. This plasmid would also contain a second selection marker and a sequence to facilitate conjugation as a means of transformations. To this end, we have cloned the aforementioned antibiotic selection marker and flanking sequences into the vector pSET151 that contains an *oriT* sequence and a second antibiotic resistance marker. In future studies, we shall use this vector to disrupt the *oxyT* gene and determine whether

this mutant produces 4-amino-anhydrotetracycline. If it does produce this compound, then we shall use this compound for characterization of OxyT. Furthermore, chelocardin is a tetracycline antibiotic that resembles 4-amino-anhydrotetracycline (Figure 2.7). It is produced as a natural product by *Amycolatopsis sulphurea*, and we also intend to purify this compound and determine whether OxyT can catalyze the methylation of this compound.

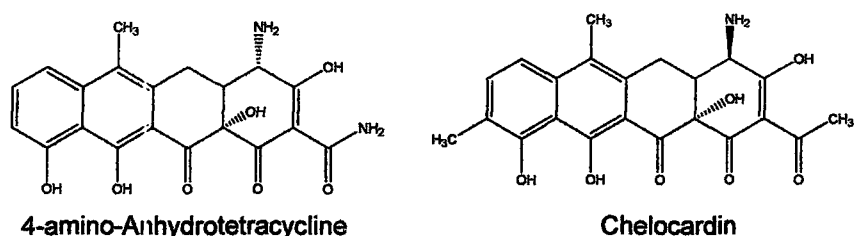


Figure 2.7. Chemical structures of 4-amino-anhydrotetracycline and chelocardin.

Reference List

Brodersen, D.E., Clemons, W.M., Jr., Carter, A.P., Morgan-Warren, R.J., Wimberly, B.T., and Ramakrishnan, V. (2000). The structural basis for the action of the antibiotics tetracycline, pactamycin, and hygromycin B on the 30S ribosomal subunit. *Cell* *103*, 1143-1154.

Burdett, V. (1991). Purification and characterization of Tet(M), a protein that renders ribosomes resistant to tetracycline. *J. Biol. Chem.* *266*, 2872-2877.

Chopra, I. and Roberts, M. (2001). Tetracycline antibiotics: mode of action, applications, molecular biology, and epidemiology of bacterial resistance. *Microbiol. Mol. Biol. Rev.* *65*, 232-260.

Gust, B. REDIRECT^(c) technology: PCR-targeting system in *Streptomyces coelicolor*. Kieser, T. Chater K. F. 1-40. 2002. Norwich, U.K., John Innes Centre.
Ref Type: Generic

Hertweck, C., Luzhetskyy, A., Rebets, Y., and Bechthold, A. (2007). Type II polyketide synthases: gaining a deeper insight into enzymatic teamwork. *Nat. Prod. Rep.* *24*, 162-190.

Hinrichs, W., Kisker, C., Duvel, M., Muller, A., Tovar, K., Hillen, W., and Saenger, W. (1994). Structure of the Tet repressor-tetracycline complex and regulation of antibiotic resistance. *Science* *264*, 418-420.

Invitrogen. Gateway Technology. A[12535-019]. 9-20-2003. Invitrogen.
Ref Type: Catalog

Lai, J.R., Koglin, A., and Walsh, C.T. (2006). Carrier protein structure and recognition in polyketide and nonribosomal peptide biosynthesis. *Biochemistry* *45*, 14869-14879.

Pioletti, M., Schlunzen, F., Harms, J., Zarivach, R., Gluhmann, M., Avila, H., Bashan, A., Bartels, H., Auerbach, T., Jacobi, C., Hartsch, T., Yonath, A., and Franceschi, F. (2001). Crystal structures of complexes of the small ribosomal subunit with tetracycline, edeine and IF3. *EMBO J.* *20*, 1829-1839.

Ross, J.I., Eady, E.A., Cove, J.H., and Cunliffe, W.J. (1998). 16S rRNA mutation associated with tetracycline resistance in a gram-positive bacterium. *Antimicrob. Agents Chemother.* *42*, 1702-1705.

Yang, W., Moore, I.F., Koteva, K.P., Bareich, D.C., Hughes, D.W., and Wright, G.D. (2004). TetX is a flavin-dependent monooxygenase conferring resistance to tetracycline antibiotics. *J. Biol. Chem.* *279*, 52346-52352.

Zakeri, B. and Wright, G.D. (2008). Chemical biology of tetracycline antibiotics. *Biochem. Cell Biol.* 86, 124-136.

**CHAPTER 3: INVESTIGATION OF A GLYCOPEPTIDE
METHYLTRANSFERASE**

Investigation of A Glycopeptide Methyltransferase

3.1. Introduction

Glycopeptide antibiotics were first introduced into the clinic over half a century ago. They are narrow spectrum antibiotics that are active against Gram-positive bacteria. The most prominent member of this class of antibiotics, vancomycin, was initially reserved for use as a last resort for treatment of Gram-positive infections due to toxicity issues related to the purity of the drug and the availability of more favoured β -lactam antibiotics (Pace and Yang, 2006; Levine, 2008). However, the emergence of multidrug-resistant staphylococci and in particular methicillin-resistant *Staphylococcus aureus* (MRSA) lead to an increased use of glycopeptides (vancomycin and teicoplanin) (Pace and Yang, 2006). As a result, tolerant and resistant bacteria began to appear, highlighting the need for the development of new glycopeptides.

Glycopeptides are bactericidal antibiotics that function by inhibiting peptidoglycan biosynthesis. They do so by binding D-Ala-D-Ala termini of uncross-linked peptidoglycan pentapeptides and thus interfering with the function of transpeptidases and transglycosylases (Pootoolal et al., 2002). In order to combat the effects of these antibiotics, bacteria have evolved a complex resistance mechanism that restructures the cell wall. In resistant bacteria, the D-Ala-D-Ala termini are converted to D-Ala-D-Lactate for which glycopeptides have a 1000-fold reduced affinity (Hubbard

and Walsh, 2003). Thus, in order to maintain the clinical efficacy of glycopeptides we must seek novel derivatives that can evade acquired antibiotic resistance.

The biosynthetic cluster of chloroeremomycin, a glycopeptide antibiotic, contains a methyltransferase enzyme that has since been called MtfA (van Wageningen et al., 1998). In 2000, O'Brien et al. demonstrated that MtfA is an N-methyltransferase that is capable of methylating different glycopeptide scaffolds such as N-demethylvancomycin, the aglycone of N-demethylvancomycin, and the linear heptapeptide of vancomycin (O'Brien et al., 2000). Therefore, with the ability to modify different glycopeptides we may be able to utilize MtfA as an agent to increase the chemical diversity of this class of compounds. In this regard, MtfA has been previously used in our laboratory by Dr. Sherry Lamb for modification of the glycopeptide A47934.

Streptomyces toyocaensis produces the antibiotic A47934 and previously in our laboratory, we have constructed a mutant that lacks the sulfotransferase *staL*, which subsequently produces desulfo-A47934 (Fig. 3.1). In earlier work, Dr. Sherry Lamb characterized the activity of MtfA *in vivo* demonstrating that it is able to methylate the N-terminal amino acid of desulfo-A47934 but not A47934 (Lamb, 2007) (Fig. 3.2). Herein, our objectives are to characterize MtfA *in vitro*. Through collaboration with a group at the National Research Council of Canada, the crystal structure of MtfA had been determined previously. Our intentions are to perform biochemical studies on MtfA and four of its mutants with alterations in key residues in order to gain a better understanding of the enzyme.

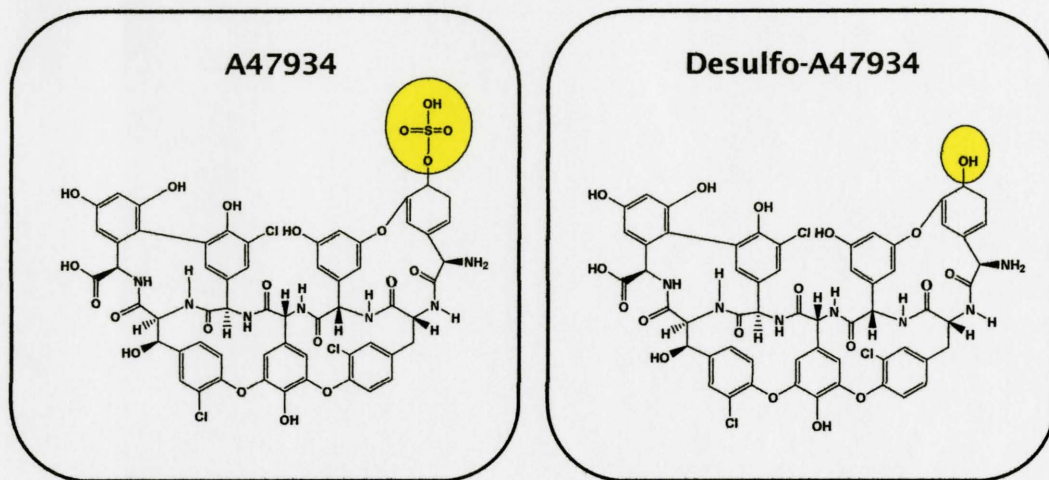


Figure 3.1. The structures of A47934 and desulfo-A47934. A47934 is produced by *S. toyocaensis*, and desulfo-A47934 is produced by the mutant *S. toyocaensis* Δ staL which lacks a sulfotransferase. The yellow circles highlight the difference between the two compounds.

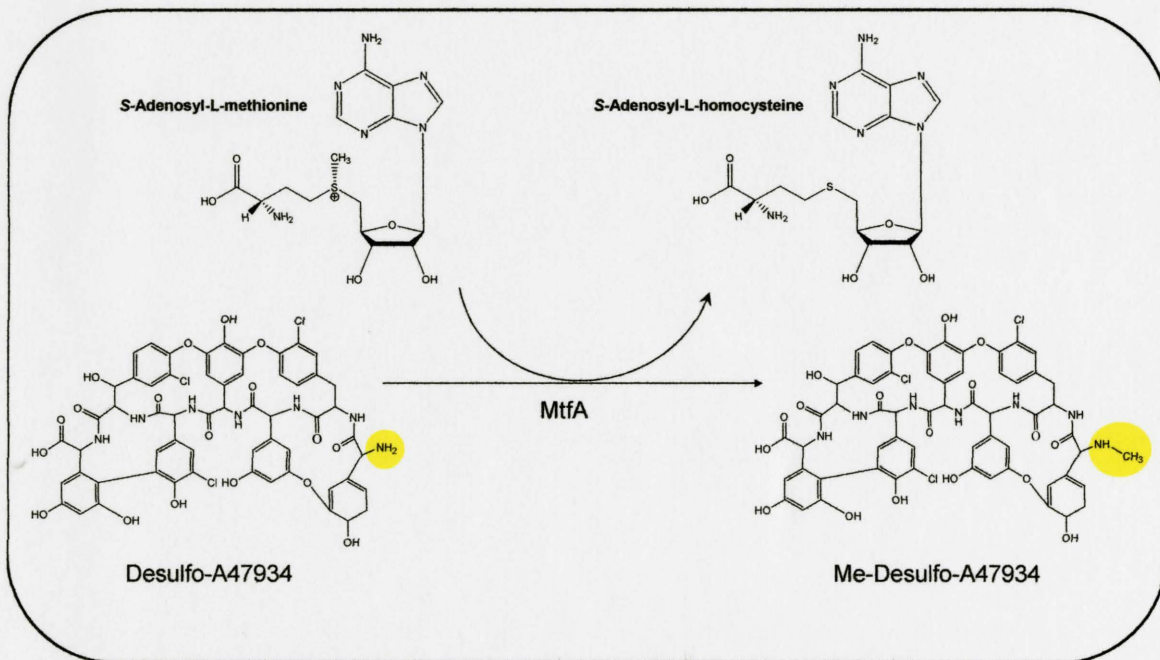


Figure 3.2. The methylation reaction catalyzed by MtfA. MtfA utilizes S-adenosyl-L-methionine as a methyl donor to methylate the N-terminal amino acid of desulfo-A47934 to produce Me-desulfo-A47934.

3.2. Materials and Methods

3.2.1. Amplification and Cloning of *mtfA* Mutants

A pET28a-*mtfA* construct was used as a template for site-directed mutagenesis to construct four mutants with single amino acid alterations (Y32F, E144A, H228A, and R230A). The protocol used was based on the QuikChange[®] site-directed mutagenesis kit (Stratagene). The primers used for site-directed mutagenesis are shown in Table 3.1. The PCR conditions used in a 50 μ L reaction are: ~55 ng pET28a-*mtfA*, 125 ng of forward and reverse primers, 0.8 mM dNTPs, 5% dimethyl sulfoxide, 4 mM MgCl₂, and 2.5 U Stratagene PFU Ultra. The PCR program used was (annealing temperatures used are shown in Table 3.1): 95°C for 3 min, (95°C for 1 min, annealing temperature for 1 min, 68°C for 7 min), and 68°C for 15 min. The PCR products were treated with 10 U of *Dpn I* for 1 hour at 37°C and transformed into *E. coli* TOP10 cells using electroporation. Products were analyzed by complete gene sequencing to ensure the desired mutations were introduced.

Table 3.1. PCR primer details for site-directed mutagenesis on pET28a-*mtfA*. These primers were used to construct four mutants of MtfA, each with a single residue alteration.

MtfA Mutant	Primer Direction	Primer Sequence	Annealing Temperature
Y32F	Forward	5'-gtgctgtgcgacttcttcgacgagggcg-3'	61°C
	Reverse	5'-cgccctcgtcgaagaagtcgcacagcac-3'	61°C
E144A	Forward	5'-ggctc gatcaacgcactggacgaggcc-3'	63°C
	Reverse	5'-ggcctcgtccagtgcgtgatcgagcc-3'	63°C
H228A	Forward	5'-tcgtcgtgtgcacggctcgcagaaggctcc-3'	63°C
	Reverse	5'-ggagccttctgcgagccgtgcacacgacga-3'	63°C
R230A	Forward	5'-tgtgcacgcacgcgcaaggctcctcgcac-3'	60°C
	Reverse	5'-gtgcgaggagccttgcgcgatgcgtgcaca-3'	60°C

3.2.2. Purification of MtfA and Its Mutants

Wild-type *mtfA*, *mtfA* Y32F, E144A, H228A, and R230A genes contained in the expression vector pET28a containing an N-terminal 6X His tag, were transformed in to *E.coli* BL21(DE3) cells using electroporation. These constructs were grown overnight in Luria-Bertani (LB) media (50 µg/mL kanamycin). 10 mL of overnight cultures were used to inoculate 1 L of LB media (50 µg/mL kanamycin) and cultures were growth at 37°C and 250 rpm until an OD₆₀₀ of ~0.6. Subsequently, IPTG (1 mM final concentration) was added to the cultures and they were grown overnight at 16°C and 240 rpm. Cultures were centrifuged (5000g for 20 min on a Beckman Coulter Avanti™ J-25 centrifuge), then

pellets were re-suspended in 20 mL 0.85% (w/v) saline and centrifuged again (3000 rpm for 20 min) and pellets were stored at -80°C.

Cell pellets were lysed using a French Press (Thermo Electron Corporation French Press Cell Disruptor), lysates were centrifuged at 18000 rpm for 30 min at 4°C and supernatants were immediately applied to a Ni-NTA column with a ~2 mL bed volume (Qiagen Canada). Lysates were washed with 50 mM NaH₂PO₄ and 300 mM NaCl buffer pH 8.0 with increasing amounts of imidazole (10 mM, 20 mM, and 50 mM), and protein was eluted with 250 mM imidazole. Protein fractions were analyzed on a 15% SDS-polyacrylamide gel and fractions containing MtfA were pooled and dialyzed against 50 mM NaH₂PO₄ pH 8.0. Protein concentration was determined using a Bradford assay (reagent from Bio-Rad Laboratories).

3.2.3. Purification of desulfo-A47934

S. toyocaensis Δ staL was cultivated in 25 mL of *Streptomyces* Vegetative Media (SVM) (Per 100 mL of media: 1.5 g glucose, 2.0 g potato starch, 1.5 g ground soygrits, 1.0 g yeast extract, 0.2 g CaCO₃, 1.0 mL corn steep liquor, pH to 6.5) in a 50 mL Erlenmeyer flask containing an ~2 cm spring for aeration, and incubated at 30°C for 2 days. Subsequently, 500 μ L was used to sub-culture 50 mL of *Streptomyces* Antibiotic Media (SAM) (Per 1 L media: 15.0 g glucose, 15.0 g soytone, 5.0 g NaCl, 1.0 g yeast extract, 1.0 g CaCO₃, 2.5 mL glycerol, pH 6.8) in a 250 mL Erlenmeyer flask containing circularized springs (~5 cm) for increased aeration and incubated at 30°C for 6 days. The cultures were then centrifuged (3000 rpm for 10 min on a Sorvall RT 6000B centrifuge) and the wet weight of the pellet was determined for antibiotic extraction using a

modification of a protocol described in (Boeck and Mertz, 1986) (supernatants were stored at -20°C).

For antibiotic extraction from wet cell pellets, 500 µL of 1% (v/v) NH₄OH was added per 1 g of cell mass. The pellets were vigorously vortexed and centrifuged (3000 rpm for 10 min), and the pH of supernatant was adjusted to 7.5 using 1 M HCl. The extracts were then tested by disk-agar diffusion for the presence of antibiotic. Briefly, a sample containing *Bacillus subtilis* 1A1 at an OD₆₂₅ of 0.08-0.1 was used to streak a lawn of bacteria on Tryptone Soya Agar plates (Per 500 mL of media: 15.0 g of Oxoid tryptone soya broth powder CM129, 7.5 g agar). Then sterile antibiotic disc were placed on the plate and 20 µL of each extract was added to check for the presence of a zone of inhibition of growth (plates were incubated at 30°C for 2 days).

Desulfo-A47934 was purified from the extracts by fractionation through a reverse phase-medium performance liquid chromatography (RP-MPLC) column (85 mL column containing octadecyl-functionalized silica gel obtained from Sigma-Aldrich Canada Ltd.). Approximately 10 mL of extracts (pooled fractions) were applied to the column. The column was first washed with 100 mL of distilled H₂O, and then a 5-50% (v/v) acetonitrile gradient was established at a flow rate of 3 mL/min using a FMY Lab Pump Model QSY (Fluid Metering, Inc.). Fractions were collected (3 mL) and analyzed for the presence of desulfo-A47934 by absorbance readings at 220 nm and 280 nm, where fractions exhibiting high absorbance were further analyzed by liquid chromatography/mass spectrometry (LC/MS). For LC/MS (Agilent 1100 Series HPLC, Applied Biosystems QTRAP LC/MS/MS, Analyst Software 4.0) analysis, samples were

run through a Agilent ZORBAX Eclipse XD8-C8 column with solvent A containing H₂O with 0.05% formic acid and solvent B containing acetonitrile with 0.05% formic acid (Program: 0-5 min 95% A and 5% B, 25 min 3% A and 97% B, 28 min 3% A and 97% B, 30-32 min 95% A and 5% B). Desulfo-A47934 containing fractions were pooled, lyophilized (VirTis Lyo-Centre, SP Industrial Company), and subsequently re-suspended in 500 µL of 50% acetonitrile for further purification by RP-HPLC.

In order to remove contaminants from the purified desulfo-A47934, it was further purified by RP-HPLC (DIONEX GP40 HPLC). For RP-HPLC analysis, samples were run through a Grace Vydac #126 C18 column with solvent A containing H₂O with 0.1% trifluoroacetic acid and solvent B containing acetonitrile with 0.07% trifluoroacetic acid (Program: 0-5 min 100% A and 0% B, 15 min 50% A and 50% B, 20 min 0% A and 100% B, 22 min 100% A and 0% B). Fractions corresponding to desulfo-A47934 were collected, pooled, tested by LC/MS and lyophilized as before.

3.2.4. Determination of Extinction Co-efficient

RP-HPLC purified desulfo-A47934 was weighed and re-suspended in 50% acetonitrile. Using a quartz cuvette of path length 1 cm, an absorbance spectrum (200-700 nm) of desulfo-A47934 was determined on a CARY 300 Bio spectrophotometer. A peak absorbance at 280 nm was used to calculate the extinction co-efficient of desulfo-A47934 using the Beer-Lambert Law:

$$A = \epsilon bc$$

Where;

A = absorbance, ϵ = extinction co-efficient ($L \cdot mol^{-1} \cdot cm^{-1}$), b = path length (cm),

and c = concentration ($\text{mol}\cdot\text{L}^{-1}$)

3.2.5. Enzyme Activity Assays

In order to demonstrate that MtfA does add a methyl group to desulfo-A47934, the following reaction was set up: 50 mM HEPES buffer pH 7.5, 0.5 mM SAM, 50 μM desulfo-A47934, and 12 μg of wild-type MtfA in a 100 μL reaction incubated for 24 hours at 30°C. The enzymatic reactions were analyzed by LC/MS as in section 3.2.2.

The progress of enzymatic reactions was followed by RP-HPLC by measuring the area under the curve (AUC) of peaks at 280 nm. Initially, a standard curve of desulfo-A47934 concentration versus AUC was determined. Enzymatic reactions were set up as follows: 50 mM HEPES buffer pH 7.5, 0.5 mM SAM, 50 μM desulfo-A47934, and 3 μg of enzyme in a 50 μL reaction incubated for 24 hours at 30°C. Reactions were stopped by adding 1 volume of 1% trifluoroacetic acid and analyzed by RP-HPLC as in section 3.2.3 except an Agilent ZORBAX Eclipse XD8-C8 column was used. A Chromeleon 6.50 software was used to analyze the RP-HPLC data and to calculate the AUC.

3.2.6. Circular Dichroism Analysis of MtfA Wild-Type and Mutants

MtfA wild-type, Y32F, E144A, H228A, and R230A were analyzed by circular dichroism to study changes in protein structure. Protein concentrations were adjusted to 0.19 mg/mL in 50 mM NaH_2PO_4 buffer pH 8.0 with 5% glycerol. 250 μL of protein was added to a 1 mm Hellma quartz cell (minimum wavelength of 175 nm) at 25°C and sample measurements were taken every 1 nm at an average time of 3 seconds in a 195-260 nm spectrum using an AVIV 410 Circular Dichroism Spectrometer. Data are

adjusted to be expressed as mean residue ellipticity ($\text{degrees}\cdot\text{cm}^2\cdot\text{dmole}^{-1}$), and technical assistance was provided by Dr. Raquel Eband.

3.2.7. Analytical Gel Filtration of MtfA Wild-Type and Mutants

MtfA wild-type, Y32F, E144A, H228A, and R230A were analyzed by gel filtration to assess quaternary structure. The experiments were performed on an AmershamPharmaciaBiotech ÄKTA FPLC UPC-900 using a Superdex 200 HR 10/30 gel filtration column and analyzing data with Unicorn 4.12 software. To calibrate the column, Sigma Gel Filtration Molecular Weight Markers MW-GF-200 were used (Table 3.2 summarizes the protein standards, their molecular weight, and the concentrations used to load the gel filtration column). To calculate the standard curve, a plot of the logarithm of molecular weight versus the elution volume/void volume (V_e/V_0) of each protein was used. All proteins (standards and samples) were stored in 50 mM NaH_2PO_4 buffer pH 8.0 with 5% glycerol, and the running buffer used contained 50 mM NaH_2PO_4 buffer pH 8.0 and 200 mM NaCl. To load columns, 200 μL of sample was injected onto the column at a flow rate of 0.2 mL/min for 3 injection volumes and subsequently the flow rate was adjusted to 0.5 mL/min. The concentrations of MtfA proteins loaded on to the column were as follows: MtfA wild-type at 1.3 mg/mL, MtfA Y32F at 1.9 mg/mL, MtfA E144A at 1.2 mg/mL, MtfA H228A at 1.8 mg/mL, and MtfA R230A at 1.7 mg/mL.

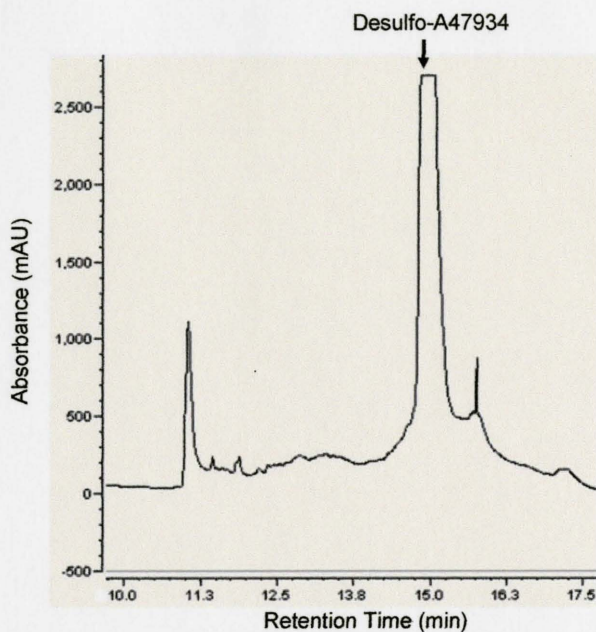
Table 3.2. A summary of the protein standards used to calibrate the Superdex 200 HR 10/30 gel filtration column. The protein standards were Sigma Gel Filtration Molecular Weight Markers MW-GF-200, and their identity, molecular weight, and concentrations used to load the gel filtration column are shown.

Protein	Molecular Weight	Concentration
Blue Dextran	2000 kDa	2 mg/mL
B-Amylase	200 kDa	4 mg/mL
Alcohol Dehydrogenase	150 kDa	5 mg/mL
Bovine Serum Albumin	66 kDa	10 mg/mL
Carbonic Anhydrase	29 kDa	3 mg/mL
Cytochrome C	12.4 kDa	2 mg/mL

3.3. Results and Discussion

In earlier studies of MtfA activity, our laboratory had demonstrated that *in vitro* MtfA is unable to methylate the natural product A47934, but does methylate the modified version of this antibiotic, desulfo-A47934 (Lamb, 2007). Desulfo-A47934 is produced by the mutant strain *S. toyocaensis* Δ staL as a secondary metabolite, thus requiring us to purify this compound for our biochemical studies. Using previously determined conditions, we expressed and purified desulfo-A47934 using RP-MPLC chromatography, which provided us with a crude sample of compound containing trace contaminants present in the culture (Figure 3.3a). To facilitate further studies with desulfo-A47934, we decided to determine the extinction co-efficient of the compound so that we may be able to accurately determine compound concentrations from our crude purifications with simple absorption measurements. Consequently, we required very pure desulfo-A47934 to calculate the extinction co-efficient and as a result we further purified our crude desulfo-A47934 fractions by purifying our samples by RP-HPLC (Figure 3.3b). By obtaining relatively pure desulfo-A47934, we reliably determined the mass of our purified compound so that we would be able to calculate the extinction co-efficient of desulfo-A47934. An absorption spectrum of desulfo-A47934 was measured with peak absorbencies at 220 nm and 280 nm (Figure 3.4). Using the peak A_{280} reading and the Beer-Lambert Law, we calculated an extinction co-efficient of $4200 \text{ Lmol}^{-1}\text{cm}^{-1}$. Vancomycin-hydrochloride, a glycopeptide antibiotic, has a similar extinction co-efficient of $4000 \text{ Lmol}^{-1}\text{cm}^{-1}$ at 280 nm (as reported by Sigma-Aldrich Canada: <http://www.sigmaaldrich.com/sigma/product%20information%20sheet/v1130pis.pdf>).

a)



b)

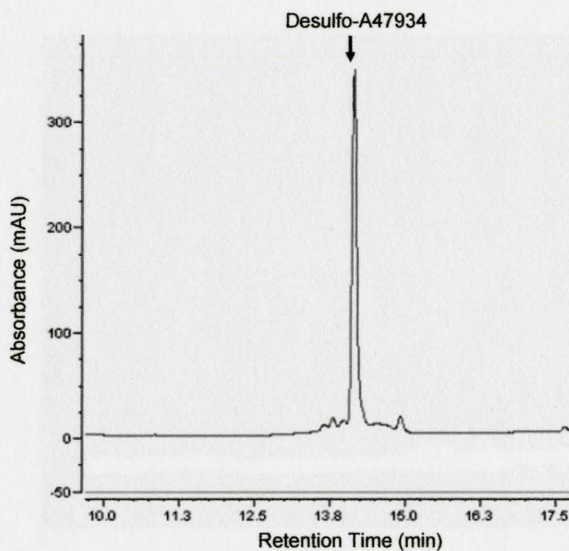


Figure 3.3. Purification of crude desulfo-A47934 by RP-HPLC. a) A crude sample of desulfo-A47934 run on a Grace Vydac #126 C18 column where desulfo-A47934 has a retention time of ~15 min. b) A purified sample of desulfo-A47934 at a concentration of 100 μ M run on an Agilent ZORBAX Eclipse XD8-C8 column where desulfo-A47934 has a retention time of ~14 min.

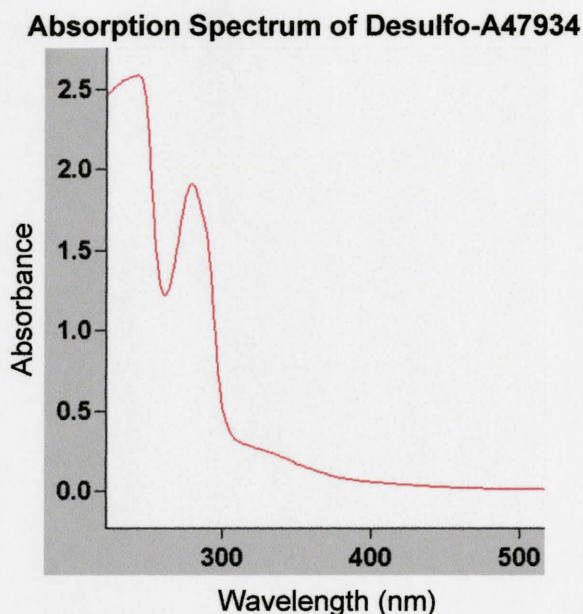


Figure 3.4. Absorption spectrum of desulfo-A47934. The absorption spectrum of desulfo-A47934 was measured from 200-700 nm with peak absorbencies at 220 nm and 280 nm. The A_{280} value was used to calculate an extinction co-efficient of $4200 \text{ Lmol}^{-1} \text{ cm}^{-1}$.

MtfA is an interesting enzyme because it is able to catalyze the methylation of certain glycopeptide scaffolds other than its natural substrate. This demonstrates its potential for glycopeptide modifications that will increase the chemical diversity of this class of antibiotics. Consequently, this enzyme warrants an in-depth study of its *in vitro* activity, which will be facilitated through crystallographic studies and enzymology. The crystal structure of MtfA bound to SAM and SAH had been previously determined in collaboration with a group at the National Research Council of Canada (Dr. Rong Shi, Dr. Allan Matte, and Dr. Mirek Cygler). The structures of MtfA-SAM and MtfA-SAH

had been determined to 2.67 and 2.95 Å resolution, respectively (Lamb, 2007). Through analysis of the crystal structure and docking models of desulfo-A47934 in the substrate binding site of MtfA, our collaborators identified four residues that may play key roles in substrate binding and catalysis (Y32, E144, H228, and R230). The relative orientation of these residues in relation to SAM and desulfo-A47934 are shown in figure 3.5. E144 interacts with the adenine ring of SAM, while Y32, H228, and R230 interact with desulfo-A47934. To study the importance of these residues, we made four corresponding single residue alterations of MtfA and characterized these mutants along with MtfA wild-type through *in vitro* studies. In addition, the docking models created illustrate the close proximity of the methyl donating sulfur moiety of SAM and the methyl receiving N-terminal amino acid of desulfo-A47934 (Figure 3.5). The SAM molecule is curved in order to readily provide the methyl moiety for transfer.

A pET28a-MtfA plasmid containing an N-terminal 6X His-tag was used as a template for site-directed mutagenesis to generate the four mutants: Y32F, E144A, H228A, and R230A. The four constructed mutants were sequenced to ensure the correct mutations had been introduced. Subsequently, the plasmids were transformed into *E. coli* BL21(DE3) cells for protein expressions. The expressed proteins were purified using Ni-NTA column chromatography, all yielding a protein of approximately ~36 kDa. Proteins were dialyzed against 50 mM NaH₂PO₄ pH 8.0 buffer, 5% glycerol stocks were made and stored at -80°C.

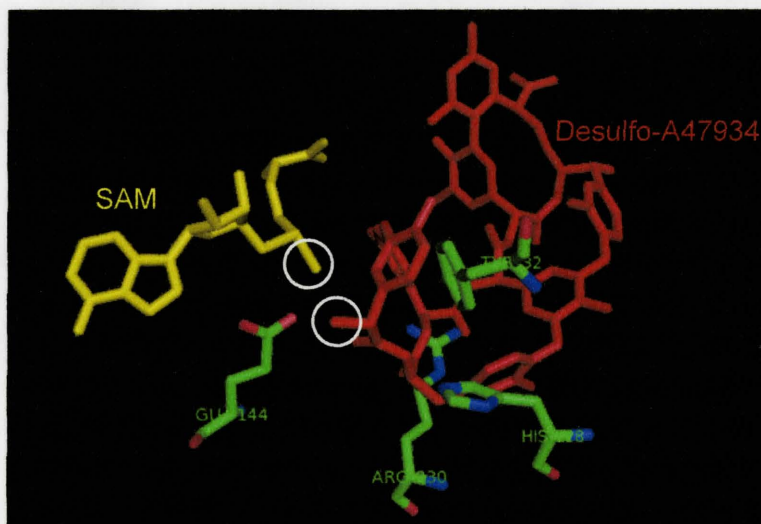


Figure 3.5. SAM and desulfo-A47934 bound to the substrate binding site of MtfA. Based on structural studies, it is believed that Tyr-32, Glu-144, His-228, and Arg-230 play key roles in substrate binding and catalysis. The white circles highlight the methyl donating and receiving regions of SAM and desulfo-A47934, respectively. This figure was generated using PyMOL v.0.99.

For enzymatic characterization of MtfA, we first had to demonstrate that MtfA can catalyze the transfer of a methyl group to the substrate desulfo-A47934. To do so, enzymatic reactions were setup and analyzed by LC/MS (results are shown in figure 3.6). LC/MS analysis of the control reaction without added enzyme shows a single molecule with an m/z of 1233.2 corresponding to desulfo-A47934 (Figure 3.6a). However, in the presence of wild-type MtfA, a new molecule with an m/z of 1247.4 appears with a mass difference of 14 as compared to desulfo-A47934 (Figure 3.6b). An increase in mass of 14 corresponds to a loss of one hydrogen atom and an addition of one methyl group, which confirms that MtfA does catalyze the methylation of desulfo-A47934.

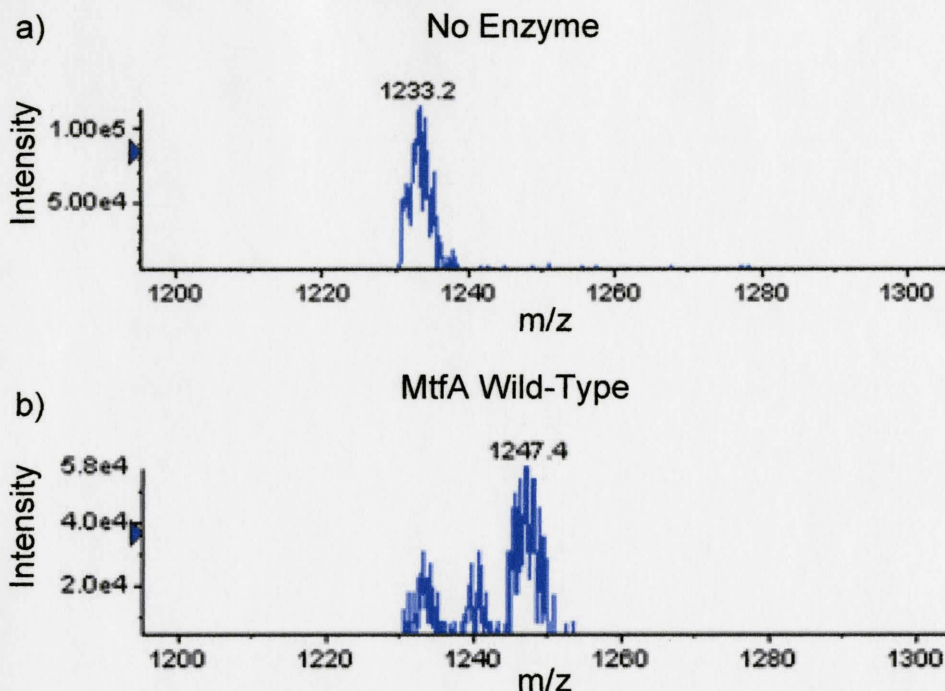


Figure 3.6. Wild-type MtfA methylation of desulfo-A47934. The following reactions were setup and analyzed by LC/MS: 50 mM HEPES buffer pH 7.5, 0.5 mM SAM, 50 μ M desulfo-A47934, and no enzyme (a) or 12 μ g of wild-type MtfA (b). Reactions were incubated at 30°C for 24 hours.

To evaluate the potential of MtfA for use as an agent for modifying glycopeptide scaffolds, we had to study the kinetics of the methylation reaction. Due to a lack of an appropriate assay for detection of desulfo-A47934 methylation, we used RP-HPLC to measure the extent of methylation. RP-HPLC is a very sensitive technique and we calibrated our system by generating a standard curve to assess the reproducibility of using this method of detection (Figure 3.7). Based on the standard curve generated with an R^2 value of 0.9925 and a detection limit of up to 400 μ M desulfo-A47934, it was concluded

that this was the method of choice for quantifying the progress of our enzymatic reactions.

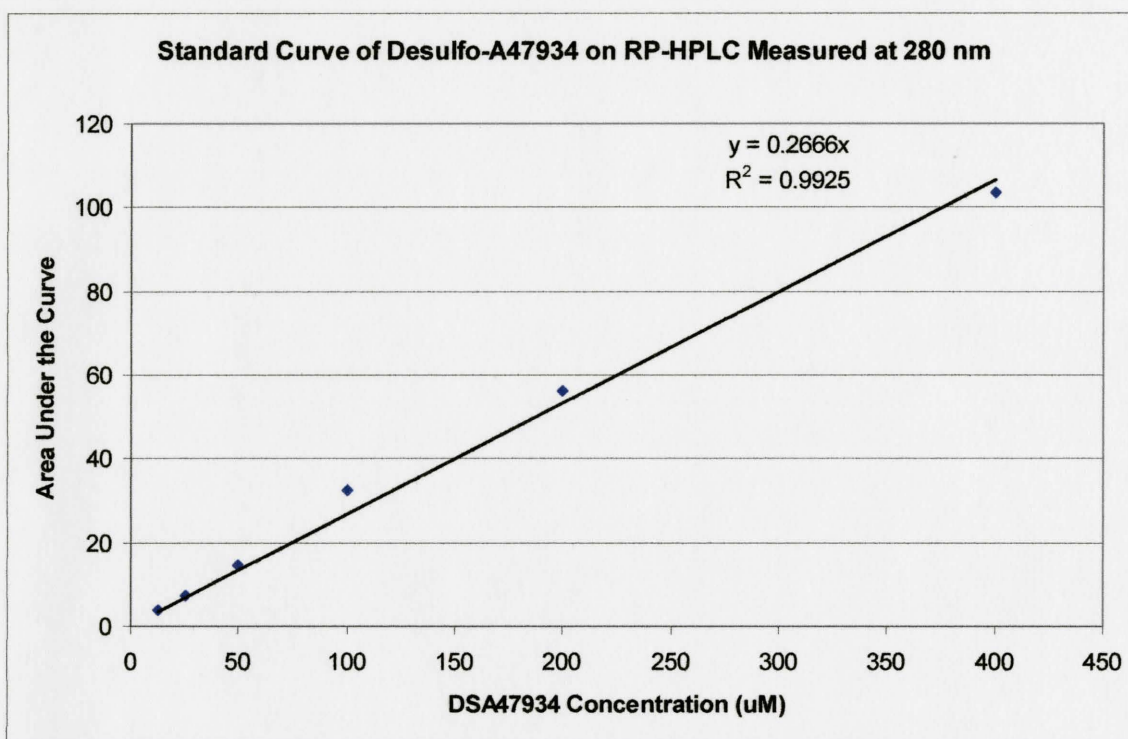


Figure 3.7. Standard curve of desulfo-A47934 on RP-HPLC measured at 280 nm. Purified desulfo-A47934 was run on an Agilent ZORBAX Eclipse XD8-C8 column in duplicate and area under the curve was used to quantify compound concentration.

Initially we intended to calculate the kinetic parameters of MtfA wild-type and its four mutants. However, our preliminary studies demonstrated that MtfA wild-type reactions *in vitro* are very inefficient and are too slow to reliably calculate kinetic parameters. Consequently, to assess reaction progression we decided to calculate the percent conversion of substrate to product in a 24 hour incubation period. Enzymatic reactions of MtfA wild-type, Y32F, E144A, H228A, and R230A were prepared in duplicate as follows: 50 mM HEPES buffer pH 7.5, 0.5 mM SAM, 50 μ M desulfo-A47934, and 3 μ g of enzyme (incubate for 24 hours at 30°C). Reactions were stopped by the addition of one volume of 1% trifluoroacetic acid and reaction progress was quantified by RP-HPLC (Figure 3.8). As expected, the MtfA mutants were significantly hindered in their ability to methylate desulfo-A47934 since mutations were made in important residues involved in substrate binding and catalysis. MtfA wild-type converted 50.6% of desulfo-A47934 into Me-desulfo-A47934, while MtfA R230A had the most activity among the mutants with 15.1% conversion (Table 3.3). MtfA Y32F (11.6% conversion) and MtfA E144A (9.3% conversion) had similar activity while MtfA H228A was completely inactivate. These finding demonstrated that Y32, E144, and R230 are required for efficient catalysis by MtfA and their disruption causes a significant loss of activity. However, H228 is essential for MtfA activity and its disruption leads to a catalytically inactive enzyme.

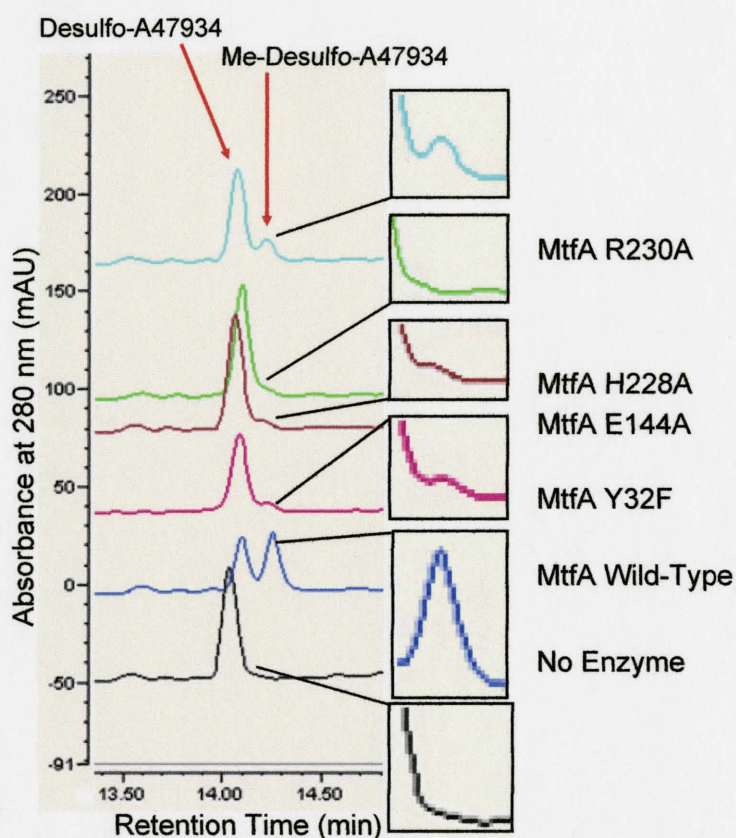


Figure 3.8. RP-HPLC analysis of desulfo-A47934 methylation by MtfA wild-type and mutants. Enzymatic reactions were prepared as follows: 50 mM HEPES buffer pH 7.5, 0.5 mM SAM, 50 μ M desulfo-A47934, and 3 μ g of enzyme (incubate for 24 hours at 30°C). Complete reactions were injected on to a RP-HPLC and reaction progress was quantified by measuring the area under the curve at 280 nm. Insets show a close up of the product peaks.

Table 3.3. Catalytic activity of MtfA wild-type, Y32F, E144A, H228A, and R230A. Enzymatic reactions were performed in duplicate and an average of the results is shown. Enzymatic activity was quantified by measuring the amount of substrate that was converted to product.

Enzyme	Average Percent Conversion	Standard Deviation
No Enzyme	0.0	0.0
MtfA Wild-Type	50.6	3.4
MtfA Y32F	11.6	1.5
MtfA E144A	9.3	2.1
MtfA H228A	0.0	0.0
MtfA R230A	15.1	4.4

The catalytic activities of the MtfA mutants were significantly reduced as compared to the wild-type enzyme. This difference in activity may either have been due to disruption of key residues involved in substrate binding and catalysis or these mutations may have lead to an alternation in global protein structure. To test whether the introduced mutations adversely affected protein folding, we analyzed the enzymes by circular dichroism and gel filtration. Circular dichroism allows us to assess the global protein folding patterns of the MtfA mutants in comparison to the wild-type enzyme. Deviations from the wild-type enzyme spectrum will inform us that the introduced mutations may have disrupted protein folding. Crystallographic analysis by our collaborators has demonstrated that MtfA is present as a homodimer. Thus, we also

intended to test whether the introduced mutations affected protein dimerization by gel filtration studies.

The global protein structure of MtfA wild-type and mutants were tested by circular dichroism analysis with an AVIV 410 Circular Dichroism Spectrometer. Proteins were stored in 50 mM NaH₂PO₄ buffer pH 8.0 with 5% glycerol and were tested at 0.19 mg/mL. Data were analyzed and reported as mean residue ellipticity (degrees·cm²·dmole⁻¹) (Figure 3.9). The mean residue ellipticity reading of MtfA Y32F, E144A, H228A, and R230A were very similar to that of the wild-type without any deviations in the spectrum produced. This demonstrated that mutations in residues Y32, E144, H228, and R230 did not lead to any significant alterations in protein folding. Thus, when these residues are disrupted the resulting reduction in activity is not due to an incorrectly folded protein.

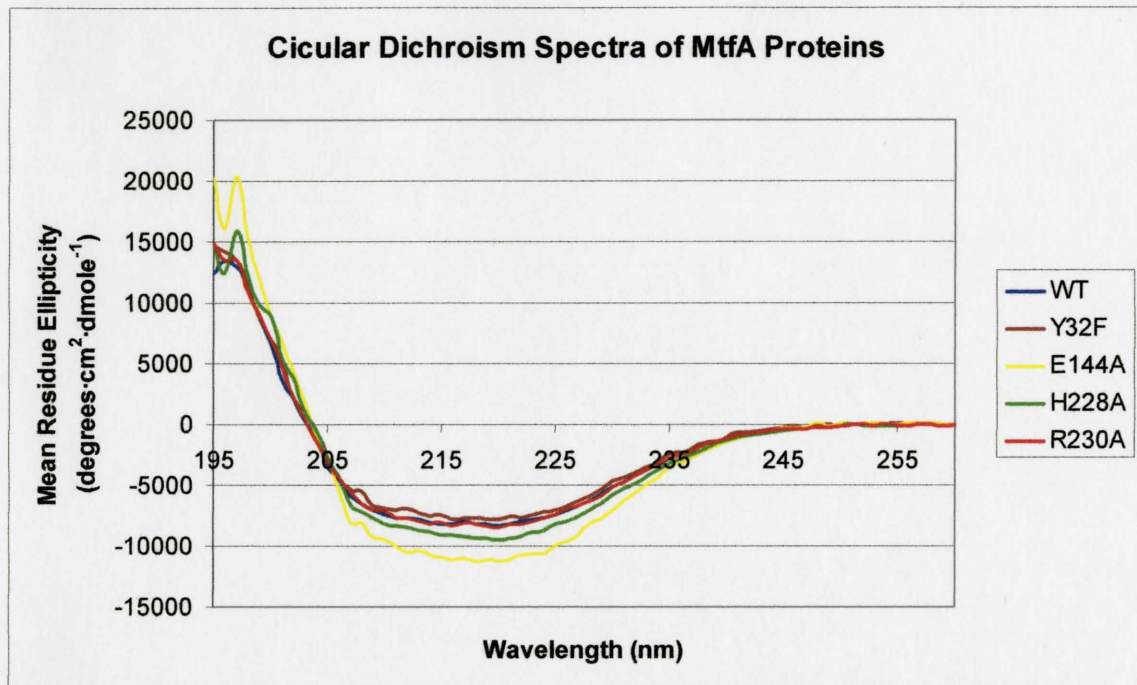


Figure 3.9. Circular dichroism spectrums of MtfA wild-type, Y32F, E144A, H228A, and R230A. Proteins were stored in 50 mM NaH₂PO₄ buffer pH 8.0 with 5% glycerol and were scanned in an AVIV 410 Circular Dichroism Spectrometer at a concentration of 0.19 mg/mL.

Gel filtration is a chromatography technique that accurately separates proteins according to their molecular size. Accordingly, a protein that is a homodimer would elute at a mass twice that of its monomer. Thus, by analyzing the MtfA proteins by gel filtration, we would be able to assess whether they are still able to dimerize after the introduced mutations. A Superdex 200 HR 10/30 gel filtration column (AmershamPharmaciaBiotech) was first calibrated with molecular weight markers (Sigma-Aldrich Co.) run in duplicate (Figure 3.10). The standard curve produced was highly reliable with an R^2 value of 0.99. Subsequently, MtfA wild-type and its mutants

were analyzed by gel filtration (in duplicate), and using the generated standard curve the molecular weight of the proteins was determined (Table 3.4). The predicted molecular weight of 6X His tagged MtfA is 32.7 kDa and thus that of the homodimer is 65.4 kDa. MtfA wild-type and Y32F both ran as proteins of 66.0 kDa molecular weight, while MtfA E144A, H228A, and R230A all ran as proteins of 69.2 kDa molecular weight. These results demonstrate that mutations in residues Y32, E144, H228, and R230 do not interfere with dimerization of MtfA. Therefore, the reduced catalytic activity of these mutants is not due to interference with dimerization.

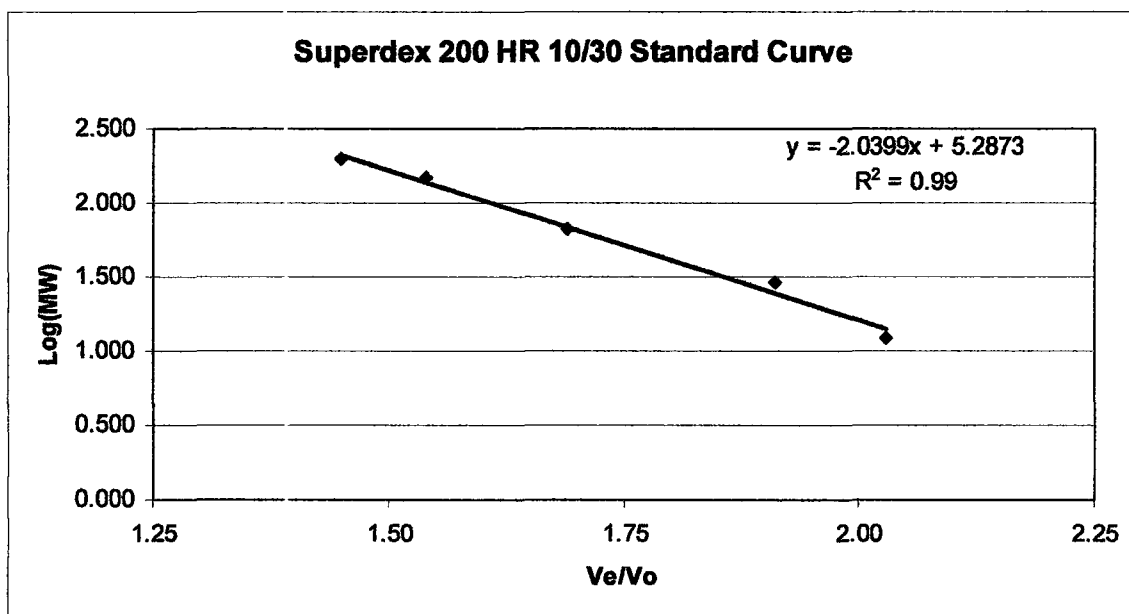


Figure 3.10. A standard curve of Superdex 200 HR 10/30 gel filtration column. The following molecular weight standards were used to calibrate the column: blue dextran (2000 kDa), β -amylase (200 kDa), alcohol dehydrogenase (150 kDa), bovine serum albumin (66 kDa), carbonic anhydrase (29 kDa), and cytochrome c (12.4 kDa). The gel filtration experiment was performed on an AmershamPharmaciaBiotech ÄKTA FPLC UPC 900.

Table 3.4. Calculation of protein molecular weights using a Superdex 200 HR 10/30 gel filtration column. The following molecular weight standards were used to calibrate the column: blue dextran (2000 kDa), β -amylase (200 kDa), alcohol dehydrogenase (150 kDa), bovine serum albumin (66 kDa), carbonic anhydrase (29 kDa), and cytochrome c (12.4 kDa). The gel filtration experiment was performed on an AmershamPharmaciaBiotech ÄKTA FPLC UPC 900.

Protein	Calculate Molecular Weight
MtfA wild-type	66.0 kDa
MtfA Y32F	66.0 kDa
MtfA E144A	69.2 kDa
MtfA H228A	69.2 kDa
MtfA R230A	69.2 kDa

3.4. Conclusions

Glycopeptides are an important class of antimicrobials that have achieved over five decades of clinical use, however emerging clinical resistance threatens their future efficacy (Levine, 2003). This highlights a need for the development of new glycopeptides that can evade resistance mechanisms. Herein, we have characterized the glycopeptide N-methyltransferase, MtfA, to gain a deeper understanding of this enzyme so that we may be able to utilize it to increase the chemical diversity of glycopeptides.

By constructing mutants of MtfA, we have been able to study important residues of the enzyme that play key roles in substrate binding and catalysis. Single residue alterations were made for amino acids Y32, E144, H228, and R230. By analyzing these mutants with circular dichroism and gel filtration experiments, we verified that these mutations did not lead to significant alterations in protein folding. Alterations in residues Y32, E144, and R230 did not lead to a complete loss of catalytic activity, while mutation of H228 abolished all catalytic activity of MtfA. Thus, these four residues are intricately involved in the methyl transfer process but do not play a significant role in protein folding or dimerization.

Based on our *in vitro* studies, MtfA was very inefficient at methylating desulfo-A47934. Therefore, its potential for *in vitro* modification of glycopeptides may be of limited use. Other options for methylating desulfo-A47934 should be sought after such as chemical modification or *in vivo* production of Me-desulfo-A47934. Previously in our laboratory, a strain of *S. toyocaensis* Δ *staL* containing an integrated copy of the *mtfA* gene was constructed. By expressing MtfA, this strain converted approximately 40% of

desulfo-A47934 into Me-desulfo-A47934 (Lamb, 2007). This process may be made more efficient by the construction of a system in a heterologous *Streptomyces* host that would lead to the sole production of Me-desulfo-A47934.

Reference List

- Boeck,L.D. and Mertz,F.P. (1986). A47934, a novel glycopeptide-aglycone antibiotic produced by a strain of *Streptomyces toyocaensis* taxonomy and fermentation studies. *J. Antibiot. (Tokyo)* *39*, 1533-1540.
- Hubbard,B.K. and Walsh,C.T. (2003). Vancomycin assembly: nature's way. *Angew. Chem. Int. Ed Engl.* *42*, 730-765.
- Lamb, S. S. Glycopeptide Antibiotics: Sulfation and Modification. 121-162. 2007. McMaster University, McMaster University.
Ref Type: Thesis/Dissertation
- Levine,D.P. (2008). Vancomycin: understanding its past and preserving its future. *South. Med. J.* *101*, 284-291.
- O'Brien,D.P., Kirkpatrick,P.N., O'Brien,S.W., Staroske,T., Richardson,T.I., Evans,D.A., Hopkinson,A., Spencer,J.B., and Williams,D.H. (2000). Expression and assay of an *N*-methyltransferase involved in the biosynthesis of a vancomycin group antibiotic. *Chem. Comm.* 103-104.
- Pace,J.L. and Yang,G. (2006). Glycopeptides: Update on an old successful antibiotic class. *Biochem. Pharmacol.* *71*, 968-980.
- Pootoolal,J., Neu,J., and Wright,G.D. (2002). Glycopeptide antibiotic resistance. *Annu. Rev. Pharmacol. Toxicol.* *42*, 381-408.
- van Wageningen,A.M.A., Kirkpatrick,P.N., Williams,D.H., Harris,B.R., Kershaw,J.K., Lennard,N.J., Jones,S.J.M., and Solenberg,P.J. (1998). Sequencing and analysis of genes involved in the biosynthesis of a vancomycin group antibiotic. *Chemistry and Biology* *5*, 155-162.

CHAPTER 4: SUMMARY

Chapter 4: Summary

4.1. Summary

We have studied two antibiotic biosynthetic methyltransferases *in vitro*. One putative methyltransferase, OxyT, is believed to be involved in the oxytetracycline biosynthetic pathway. Due to an unavailability of the predicted natural substrate for OxyT, we tested activity against commercially available compounds that resemble its natural product. However, OxyT did not display methyltransferase activity against these compounds. Possible reasons for lack of activity may be that the compounds tested are not suitable substrates for OxyT, OxyT may not have folded properly when expressed in *E. coli* Rosetta Gami pLysS, or that OxyT does not catalyze the predicted reaction of dimethylating 4-amino-anhydrotetracycline. Our attempts at disrupting the *oxyT* gene in *S. rimosus* in order to isolate 4-amino-anhydrotetracycline, OxyT's predicted natural substrate, were unfruitful. We are currently in the process of using an alternative strategy to disrupt this gene. By biochemically characterizing OxyT's activity *in vitro*, we hope to provide evidence demonstrating that this protein is indeed responsible for catalyzing the dimethylation of 4-amino-anhydrotetracycline. Also, this would shed light onto the poorly understood type II PKS pathways. Furthermore, our laboratory is interested in isolating 4-amino-anhydrotetracycline to construct novel tetracycline derivatives that can maintain their bioactivity while evading efflux dependent resistance.

The second enzyme that we studied, MtfA, is a glycopeptide methyltransferase that had been shown to methylate various glycopeptide scaffolds. Previously, our

laboratory in collaboration with a group at the National Research Council of Canada had determined the crystal structure of MtfA. Herein, we characterized MtfA and four of its mutants in order to gain a deeper understanding of this enzyme. We found that MtfA does methylate desulfo-A47934 and that residues Y32, E144, H228, and R230 play a role in catalysis but do not interfere with global protein structure or dimerization.

Based on our studies, we conclude that methyltransferases can be used as agents for increasing the chemical diversity of natural products. However, before we can take advantage of the potential of these enzymes, we must first understand their roles in natural product biosynthesis and ways of maintain their catalytic efficiency *in vitro*.

Appendix

In our attempts to inactivate the *oxyT* gene in *S. rimosus*, we constructed the plasmid pSTEA and transformed it into *S. rimosus* mycelia using electroporation. Below is outlined our materials and methods, and our screenings of putative *S. rimosus* $\Delta oxyT$ mutants.

Materials and Methods

Disruption of the *oxyT* gene in *S. rimosus*

To disrupt the *oxyT* gene in *S. rimosus*, we produced a construct called pSTEA that contains genomic sequences that flank the *oxyT* gene in *S. rimosus* positioned around an erythromycin resistance cassette from *Saccharopolyspora erythraea*. To construct pSTEA, three separate PCR products were ligated together and cloned into pDONR201 using Gateway[®] Technology in a procedure we have called “gene stitching”.

The regions flanking *oxyT* in the *S. rimosus* genome were first cloned into a plasmid we have called pSTA. To amplify the downstream sequences the following primers were used: forward primer 5' – GGGGACAAGTTTGTACAAAAAAGCAGGC TTCTCTAGAGATGCACGACGTGCGCTGGCTCTC – 3' and reverse primer 5' – GGGGAAGCTTGGAGGACGGTGCCGCCAGGTATT – 3'. To amplify the upstream sequences the following primers were used: forward primer 5' – GGGGAAGCTTGCTTCCACGGCGGCGACTTCCTGA – 3' and the reverse primer 5' – GGGGACCACTTTGTACAAGAAAGCTGGGTCTGAATTCCTCCGCCCC

GGTCGATCTTGTGA – 3'. Sequences were amplified in a 50 µL PCR reaction as follows: 0.8 mM dNTPs, 1 µL *S. rimosus* genomic DNA at a 1:10 dilution, 0.8 µM primers, 5% DMSO, 6 mM MgCl₂, and 1 U Biotools DNA polymerase. The following PCR program used: 94°C for 3 min, 30 cycles of (94°C for 1 min, 65°C, for 1 min, 72°C for 1 min), and 72°C for 10 min. PCR products were de-salted using a Qiagen PCR purification kit and 17 µL of each PCR product was digested with 20 U of HindIII enzyme at 37°C for 1 hour. Digests were de-salted using a Qiagen PCR purification kit and the PCR products were ligated as follows: 7.5 µL of each digestion reaction and 3 µL of NEB T4 DNA Ligase incubated at 16°C overnight. The following BP reaction was setup based on Gateway[®] technology (Invitrogen, 2003): 1 µL pDONR201 vector, 3 µL of ligation product, 2 µL of TE buffer pH 8.0, and 2 µL of BP Clonase Enzyme (incubate for 80 min at room temperature). The BP reaction was transformed into *E. coli* TOP10 using electroporation and plated on LB agar plates (50 µg/mL kanamycin). Colonies were screened by restriction digestion analysis and by sequencing.

pSTA was used as a template to construct the plasmid pSTEA. The downstream and upstream genomic sequences of *oxyT* were amplified as above for pSTA, where pSTA was used as the DNA template, except the primers were changed to accommodate restriction sites and the annealing temperature for the PCR program was changed to 63°C. The downstream sequence primers were: forward primer 5' – GGGGACAAGTTTGTAC AAAAAGCAGGCTTCTCTAGAGATGCACGACGTGCGCTGGCTCTC – 3' and reverse primer 5' GGGGCATATGGGAGGACGGTGCCGCCAGGTATT – 3'. The upstream sequence primers were: forward primer 5' – GGGGCTCGAGGCTTCCACGG

CGGCGACTTCCTGA – 3' and reverse primer 5' – GGGGACCACTTTGTACAAGA AAGCTGGGTTCGAATTCCCGCCCCGGTCGATCTTGTTGA – 3'. To amplify the *ermE* resistance cassette so that it would be inserted in between downstream and upstream *oxyT* sequences, the following primers were used: forward primer 5' – GGGGCATATGAGGTACGCGGCTTGCAGGTCCA – 3' and reverse primer 5' – GGGGCTCGAGTCGACCTCCGGGCCGACATCAA – 3'. The PCR reaction and program to amplify the *ermE* cassette was the same as that for pSTA except the plasmid pIJ4026 was used as the DNA template and an annealing temperature of 66°C was used. The downstream sequence PCR fragment was digested with *Nde I*, the upstream sequence PCR fragment was digested with *Xho I*, and the *ermE* cassette PCR fragment was digested with *Nde I* and *Xho I*. The digests were de-salted using a Qiagen PCR purification kit and the PCR products were ligated as follows: 7.5 µL of each digestion reaction and 3 µL of NEB T4 DNA Ligase incubated at 16°C overnight. The following BP reaction was setup based on Gateway[®] technology (Invitrogen, 2003): 1 µg pDONR201 vector, 3 µL of ligation product, 2 µL of TE buffer pH 8.0, and 2 µL of BP Clonase Enzyme (incubate for 120 min at room temperature). The BP reaction was transformed into *E. coli* TOP10 using electroporation and plated on LB agar plates (50 µg/mL kanamycin). Colonies were screened by restriction digestion analysis and by sequencing.

Electroporation of *S. rimosus*

Based on a protocol reported by Pigac and Shrempf (1995), pSTEA was transformed into *S. rimosus* mycelia using electroporation techniques. Electrocompetent

S. rimosus mycelia were produced as reported in (Pigac and Schrempf, 1995). The plasmid pSTE_A was passaged through *E. coli* GM48 to produce unmethylated DNA. To 50 µL of electrocompetent mycelia, 3 µL of unmethylated pSTE_A was added and samples were incubated on ice for 1 min. Subsequently, samples were pulsed at 2 kV for ~4 ms on a Bio-Rad Gene Pulser. Immediately, 0.75 mL of cold CRM media (Per 1 L: 10 g glucose, 103 g sucrose, 10.12 g MgCl₂·6H₂O, 15 g Oxoid Tryptone Soya Broth CM129, 5 g yeast extract) was added and samples were incubated at 30°C and 250 rpm for 3 hours. Samples were then plated on Bennet agar (Per 500 mL: 5 g potato starch, 1 g casaminoacids, 0.9 g yeast extract, 1 mL Czapek mineral mix (Per 100 mL: 10 g KCl, 10 g MgSO₄·7H₂O, 12 g NaNO₃, 0.2 g FeSO₄·7H₂O, 200 µL concentrated HCl, and 7.5 g agar) containing 50 µg/mL apramycin and 100 µg/mL erythromycin. Plates were incubated at 30°C for 4 days. Colonies were maintained in Bennet media containing 50 µg/mL apramycin and 100 µg/mL erythromycin. Spore purified mutants were screened with PCR for the presence of the *oxyT* gene using primers and conditions outlined in section 2.2.1 except with an extension time of 2.5 min for the PCR program. They were also assessed for secondary metabolic production in Bennet media containing 50 µg/mL apramycin and 100 µg/mL erythromycin (incubated for 10 days at 30°C and 250 rpm) and analyzed by LC/MS techniques described in section 2.2.3.

Results

In 2006, Yi Tang's group published the complete sequence for the biosynthetic cluster of oxytetracycline in *S. rimosus* (Zhang et al., 2006). Based on this sequence we initially decided to use REDIRECT[®] technology (Gust, 2002) to delete the *oxyT* gene. The selection markers used in this protocol provide resistance against apramycin, spectinomycin/streptomycin, and viomycin all of which *S. rimosus* is intrinsically resistant to. Therefore, we decided to use the more conventional technique of insertional inactivation of the *oxyT* gene. Accordingly, we constructed the plasmid pSTEa by sequentially ligating three PCR fragments and cloning the ligation product into pDONR201 using Gateway[®] technology (Figure A.1). pSTEa contains ~1 kb DNA sequences that correspond to the genomic sequences flanking the *oxyT* gene to aid homologous recombination. In between these sequences is an erythromycin resistance cassette containing the resistance gene *ermE* and its corresponding promoter from *S. erythraea*.

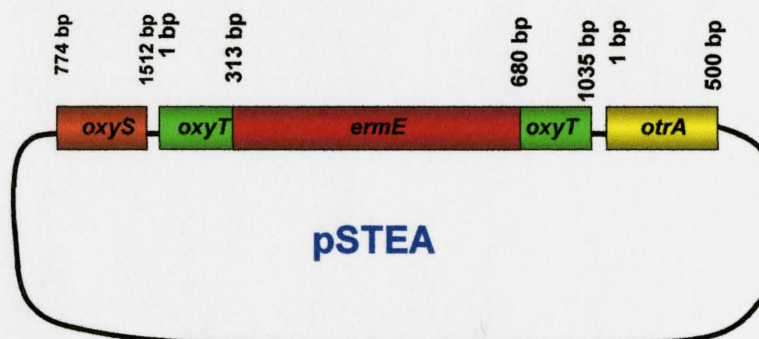


Figure A.1. Plasmid map of pSTEa. The *ermE* resistance cassette was inserted in between ~1 kb genomic sequences flanking *oxyT*. The numbers above the genes represent the sizes of the fragments of each gene that was cloned into pSTEa.

pSTEA was introduced into *S. rimosus* mycelia using a published protocol for the electroporation of *S. rimosus* by Pigac and Shremppf (1995). Subsequently, 16 putative *oxyT*-null *S. rimosus* mutants were isolated that were resistant to erythromycin. Of these 16 mutants, only 13 were stably resistant to erythromycin and thus they were cultured and spore purified. These mutants grew much slower than wild-type *S. rimosus*. In order to screen for the disruption of the *oxyT* gene, we used two different methods. Firstly, we screened for secondary metabolite production using antibiotic production conditions that we had previously determined for *S. rimosus*. If *oxyT* had been disrupted, then we would predict the mutants to produce the intermediate 4-amino-anhydrotetracycline that we could detect by LC/MS. *S. rimosus* synthesizes the compound oxytetracycline which has a molecular weight of 460.43, while the molecular weight of 4-amino-anhydrotetracycline is 398.37. Through LC/MS analysis, it was determined that all of the putative *oxyT*-null mutants produced a compound with a m/z of 460.8 that was not present in the medium control or medium containing the antibiotics used for selection and inoculated with wild-type *S. rimosus*, which does not grow in these conditions. However, this compound was present in medium inoculated with wild-type *S. rimosus* which corresponds to oxytetracycline (Figure A.2 illustrates a representative figure for one of the mutants, similar results were found for others). These findings may result from three possible outcomes, either *oxyT* was not disrupted and the erythromycin resistant *S. rimosus* mutants are drug resistant for other reasons than the introduction of the *ermE* cassette into the *oxyT* gene, or OxyT does not catalyze the hypothesized reaction, or there

is an alternative methyltransferase that can perform the reaction in the absence of *oxyT*.

To test these possibilities, we decided to use PCR techniques to amplify the *oxyT* gene in the mutants.

By using primers and similar PCR conditions used to amplify the *oxyT* gene for cloning into our expression vector, we screened several of the putative *oxyT*-null *S. rimosus* mutants to determine whether they had an intact *oxyT* gene. As mentioned earlier, these mutants grew much slower than their wild-type counterparts and therefore we managed to purify genomic DNA from only 5 mutants since the others did not provide a large enough biomass. In the PCR amplification of the *oxyT* gene, we used pSTEA as a control since it contains a disrupted *oxyT* gene and wild-type *S. rimosus* since it contains an intact *oxyT* gene. Our results demonstrated that the 5 mutants that were tested all possessed an intact *oxyT* gene just as in wild-type *S. rimosus* (Figure A.3). At this time, we decided not to perform any further tests with our *S. rimosus* mutants because they all produced oxytetracycline, while the 5 mutants tested all contained the complete *oxyT* gene.

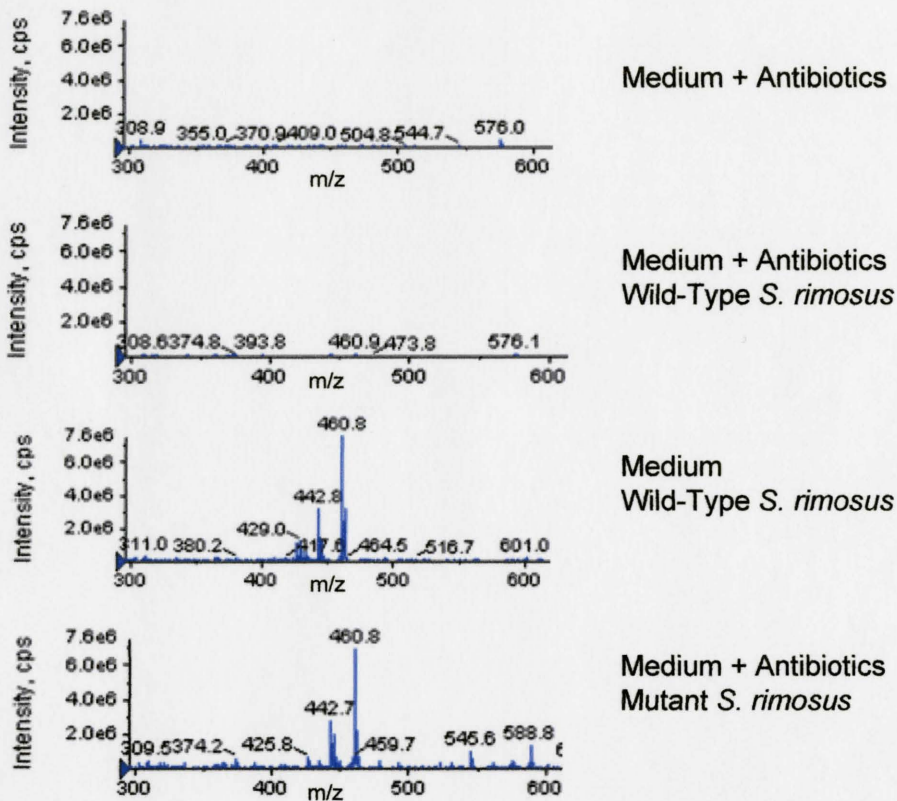


Figure A.2. LC/MS analysis of putative *oxyT*-null *S. rimosus* mutants. Cultures were grown in Bennet media containing 50 $\mu\text{g}/\text{mL}$ apramycin and 100 $\mu\text{g}/\text{mL}$ erythromycin (incubated for 10 days at 30°C and 250 rpm) and analyzed by LC/MS. The following controls were used: Bennet media containing 50 $\mu\text{g}/\text{mL}$ apramycin and 100 $\mu\text{g}/\text{mL}$ erythromycin, Bennet media containing 50 $\mu\text{g}/\text{mL}$ apramycin and 100 $\mu\text{g}/\text{mL}$ erythromycin and inoculated with wild-type *S. rimosus*, and Bennet media inoculated with wild-type *S. rimosus*. Oxytetracycline (produced by wild-type *S. rimosus*) has a molecular weight of 460.43 and 4-amino-anhydrotetracycline (intermediate predicted to be produced by *oxyT*-null *S. rimosus* mutants) has a molecular weight of 398.37.

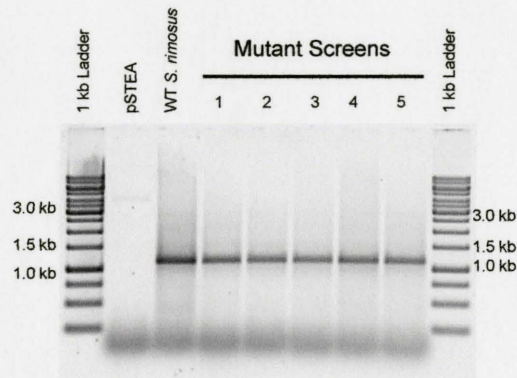


Figure A.3. PCR screening of putative *oxyT*-null *S. rimosus* mutants. The *oxyT* gene was amplified to test whether it is intact or disrupted. pSTEAs (containing a disrupted *oxyT* gene) and wild-type *S. rimosus* were used as controls. If *oxyT* was intact, a DNA fragment of ~1.1 kb was expected.

Reference List

Gust, B. REDIRECT^(c) technology: PCR-targeting system in *Streptomyces coelicolor*.
Kieser, T. Chater K. F. 1-40. 2002. Norwich, U.K., John Innes Centre.
Ref Type: Generic

Invitrogen. Gateway Technology. A[12535-019]. 9-20-2003. Invitrogen.
Ref Type: Catalog

Pigac, J. and Schrempf, H. (1995). A Simple and Rapid Method of Transformation of *Streptomyces rimosus* R6 and Other Streptomycetes by Electroporation. *Appl. Environ. Microbiol.* 61, 352-356.

Zhang, W., Ames, B.D., Tsai, S.C., and Tang, Y. (2006). Engineered biosynthesis of a novel amidated polyketide, using the malonamyl-specific initiation module from the oxytetracycline polyketide synthase. *Appl. Environ. Microbiol.* 72, 2573-2580.